The Design of Redox-Active, Olefin Polymerization Catalysts Using Late-Transition Metals

A Thesis Presented for the
Masters of Science
Degree
The University of Tennessee, Knoxville

Zachary Reynolds Sprigler

August 2013

Copyright © 2013 by Zachary R. Sprigler

All rights reserved

Acknowledgments

I would like to express my deep gratitude towards my advisor, Dr. Brian Long, for all of his support and encouragement throughout the past few years during my time in graduate school. Along with him, I want to thank the rest of my graduate committee members, Dr. Jimmy Mays and Dr. David Jenkins who have been very helpful and supportive of me as well. I want to also thank Dr. Jennifer Rhinehart and Dr. Costyl Njiojob for all of their help along the way as well as the rest of my fellow group members, Chris Bulino, Lauren Brown and Kevin Gmernicki, all of whom I would not have been successful without. Next, I want to thank Dr. Stacy O'Reilly and the rest of the Butler University chemistry department for their hard work and encouragement during my undergraduate career there. Finally, I want to thank my parents, Matt and Tracey Sprigler, as well as my brother, Corey Sprigler, for all of their love and support during this long journey. I would not have been successful without them.

Abstract

Polyolefins are the most widely produced and utilized polymers in the world. To overcome many of the obstacles associated with homogeneous, single-site catalysts, we have chosen to incorporate redox-active functionality into various ligand scaffolds. These ligand frameworks may facilitate the fine-tuning of the electronic environment around the metal center. Currently we have synthesized two new redox-active α [alpha] diimine ligands and are coordinating them with palladium-based metal precursors to give olefin polymerization catalysts. Each ligand was designed to include a different ferrocene moiety that has the ability to participate in redox chemistry. The redox capabilities of each catalyst will be examined to see if their activities can be fine-tuned in order to produce new polyolefins with new and/or enhanced mechanical properties. In addition to the α [alpha] diimine ligands, attempts to synthesize redox-active phenoxyimine ligands and one phenoxyketimine ligand, each including a different ferrocene moiety, has thus far proved elusive leading to complex product mixtures though. Currently, reaction conditions are being explored in order to isolate pure products. To compliment the ferrocenyl containing ligands above, acenaphthenequinone-based Brookhart-type ligands were also synthesized and coordinated with PdClMe(COD) [Chloromethyl(1,5-cyclooctadiene)palladium(II)] and $NiBr_2$(DME) [Nickel(II) bromide, dimethoxyethane adduct] to give previously reported olefin polymerization complexes. The redox potential of those complexes were explored using cyclic voltammetry and cobaltacene was chosen as a suitable chemical reductant. The kinetics of 1-hexene polymerization was examined using the oxidized and reduced catalysts, each of which demonstrated a different polymerization rate. In this case,

the polymerization rate of the oxidized catalyst proved to be far more active than the reduced catalyst, a phenomena that we are currently investigating.

Table of Contents

Page

Chapter 1: Introduction to Olefin Polymerization Catalysts 1

1.1: Introduction to Olefin Catalysts.....1

1.2: Development Ziegler-Natta Olefin Catalysts 2

1.3: Development of Mettalocene-Based Olefin Polymerization Catalysts 5

1.4: Development of Non-Metallocene-Based Olefin Polymerization Catalysts 7

1.5: Conclusion 10

Chapter 2: Redox-Active Olefin Polymerization Catalysts 12

2.1: Introduction.....12

2.2: Previous Research with Redox-Active Catalyst Systems.....13

2.3: Results and Discussion 18

2.4: Redox-Activity of Catalysts and Polymerizations.....27

2.5: Conclusion 37

Experimentals 29

References.....48

Appendix 52

Spectral Analysis of Compound **2.13** 53

Spectral Analysis of Compound **2.18** 56

Spectral Analysis of Compound **2.19** 58

Vita.....60

List of Tables

Table **Page**

2.1: Mass of polymer obtained and percent conversion for polymer **2.25** 31

2.2: Mass of polymer obtained and percent conversion for polymer **2.27** 35

List of Figures

Figure **Page**

1.1: U.S. polymer production in 2011 2

1.2: Karl Ziegler and Giulio Natta 3

1.3: Short segments of polypropylene showing different tacticity 4

1.4: A crystal of $TiCl_3$ used in the Ziegler-Natta catalysis of α-olefins 5

1.5: Examples of metallocene catalysts developed by Kaminsky 6

1.6: Examples of non-metallocene catalysts used for olefin polymeriation 8

1.7: Examples of FI catalysts and α-diimine catalysts 9

2.1: Overview of redox-active ligands for olefin polymerization 13

2.2: A time versus conversion graph of the hydrogenation of cyclohexene in acetone 14

2.3: Conversion versus time graph for the polymerization of *rac*-lactide 16

2.4: The redox-active metal complex studied by Diaconescu and co-workers 17

2.5: Ni(II) phenoxyimine complex developed by Grubbs 19

2.6: Cyclic voltammetry curve for PdClMe(BIAN) 27

2.7: GPC analysis of poly-1-hexene using PdClMe(BIAN) and PMAO 29

2.8: GPC analysis of poly-1-hexene using PdClMe(BIAN) and NaBArF 30

2.9: A time versus percent conversion graph for the polymerization of 1-hexene using PdClMe(BIAN) as a catalyst and NaBArf as an activator 32

2.10: A time versus conversion graph for the polymerization of 1-hexene using the reduced PdClMe(BIAN) catalyst activated with NaBArF 34

List of Figures Continued

Figure **Page**

2.11**:** A time versus percent conversion graph for the polymerization of 1-hexene showing the reduced and oxidized PdClMe(BIAN) catalyst. 35

2.10: A time versus percent conversion graph for the polymerization of 1-hexene using $NiBr_2$(BIAN) as a catalyst and PMAO as an activator....37

A.1: ^{1}HNMR spectrum for compound **2.13** 53

A.2: ^{13}CNMR spectrum for compound **2.13** 54

A.3: DART-MS spectrum for compound **2.13**....55

A.4: ^{1}HNMR spectrum for compound **2.18**....56

A.5: ^{13}CNMR spectrum for compound **2.18** 57

A.6: ^{1}HNMR spectrum for compound **2.19**....58

A.7: ^{13}CNMR spectrum for compound **2.19** 59

List of Schemes

Scheme **Page**

2.1: Redox activity of Gibson's Ti based lactide polymerization catalyst.....15

2.2: Synthesis of ethynylferrocene phenoxyimine ligand **2.8** 20

2.3: Synthesis of ethynylferrocene phenoxyimine ligand **2.11** 21

2.4: Synthesis of phenoxyketimine **2.16**.....22

2.5: Synthesis of α-diimine ligands **2.18** and **2.19** 24

2.6: Synthesis of palladium complexes **2.20** and **2.21**.....25

2.7: Synthesis of α-diimine ligand **2.22** and complexes **2.23** and **2.24** 26

2.8: The reduction of PdClMe(BIAN), **2.23**, using Cp_2Co to give catalyst **2.25** 28

2.9: The polymerization of 1-hexene using PdClMe(BIAN) to give polymer **2.26**.....28

2.11: The polymerization of 1-hexene using the reduced PdClMe(BIAN) catalysts to give polymer **2.27**.....33

2.10: The polymerization of 1-hexene using $NiBr_2$(BIAN) to give polymer **2.28**.....36

List of Abbreviations and Symbols

α .....Alpha
AcOH .....Acetic acid
AgOTF .....Silver triflate
An.....Acenaphthene group
Anth.....9-anthracene group
β .....Beta
NaBArF.....Sodium Tetrakis(3,5-bis(trifluoromethyl)phenyl)borate
BIAN.....Bis(aryl)acenaphthenequinonediimine (aryl = 2,6-diisopropylaniline)
COD .....1,5-cyclooctadiene, ligand
Cp.....Cyclopentadienyl ring, ligand
CTA.....Chain transfer agent
CV .....Cyclic voltammetry
DCM .....Dichloromethane (methylene chloride), solvent
Fc.....Ferrocene
FI .....Phenoxyimine catalyst
GPC.....Gel permeation chromatography
HDPE .....High-density polyethylene
^{i}Pr .....Isopropyl group
LDA .....Lithium diisopropyamide, used as a base in reactions
LDPE.....Low-density polyethylene
LLDPE .....Linear low-density polyethylene
MAO .....Methylaluminoxane
Me .....Methyl group
MeOH .....Methanol, solvent
M_n.....Number average molecular weight
M_w .....Weight average molecular weight
OTf.....Triflate
PDI .....Polydispersity Index
PE .....Polyethylene
Ph .....Phenyl group
Phen.....9-phenanthroline group
PMAO.....Polymethylaluminoxane-improved merformance
PP .....Polypropylene
^{t}Bu .....Tert-butyl group
THF.....Tetrahydrofuran, solvent
Tphen .....*meta*-terphenyl broup
Trityl .....Triphenylmethyl group

Chapter 1
Introduction to Olefin Polymerization Catalysts

1.1: Introduction to Olefin Catalysts

The development of polyolefinic materials such as polyethylene (PE) and polypropylene (PP) have had a profound influence on the world.[1,2,3] This is owed in part to their numerous beneficial properties such as having excellent mechanical strength, remarkable flexibility, chemical inertness and recyclability. Polyolefins are extremely lightweight when compared to traditional building materials such as wood, steel and glass and are made from some of the cheapest monomers available, such as ethylene.[2] According to the American Chemistry Council, the U.S. production of PE and PP topped 53 billion pounds in 2011, which accounts for 52 % of all U.S. polymers produced in that year (Figure 1.1).[4] It is no surprise that they are used in the production of many everyday products such as toys, bags, food packages, bottles, storage containers, car parts and even bullet-proof vests. This multitude of applications is why polyolefinic materials have become the most widely used synthetic polymers today.[5]

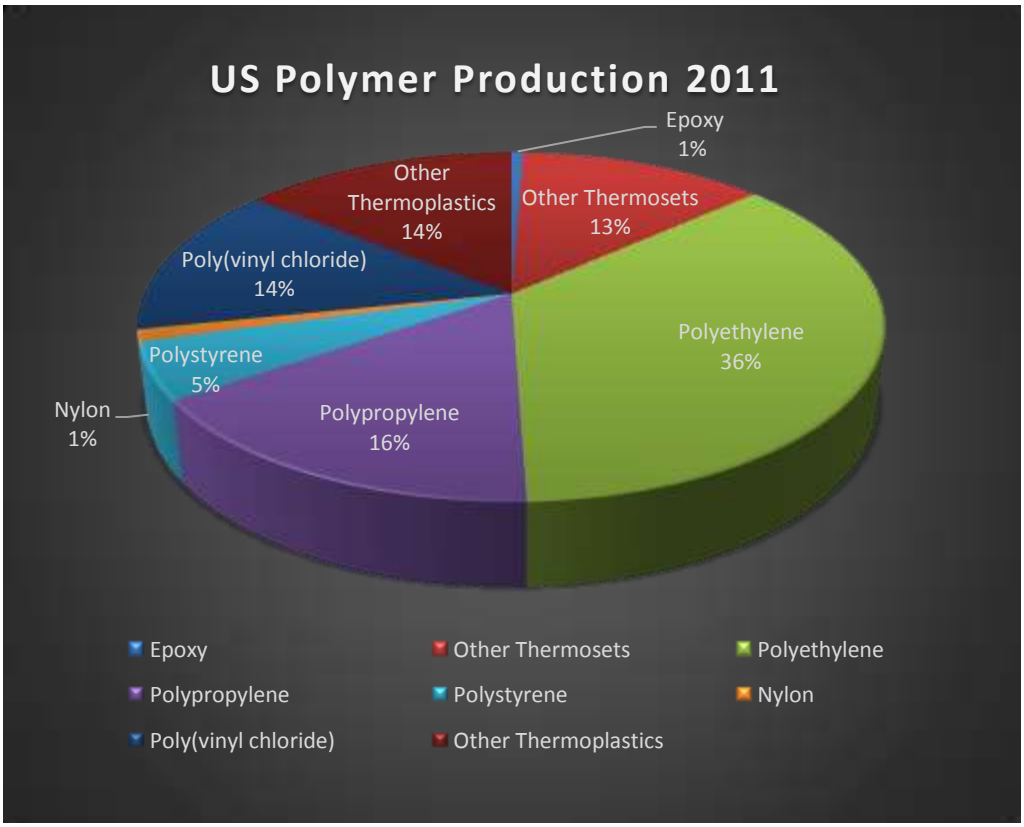


Figure 1.1. U.S. polymer production in 2011. The graph shows that PE and PP made up over half (52 %) of all polymers produced in 2011.[4]

1.2: Development of Ziegler-Natta Olefin Catalysts

In the early 1950's, Karl Ziegler (Figure 1.2)[6] discovered that certain combinations of transition metal compounds and specific organometallic reagents would polymerize ethylene at low temperatures and pressures to give polyethylene with an essentially linear structure.[7] Now known as high-density polyethylene (HDPE), this product is denser, tougher and has a higher melting temperature than the branched low-density polyethylene (LDPE) that is prepared at high pressures under free radical polymerization conditions. The low degree of branching in HDPE

leads to closer packing of the chains, thereby allowing a more regular structure and a high degree of crystallinity.[5]

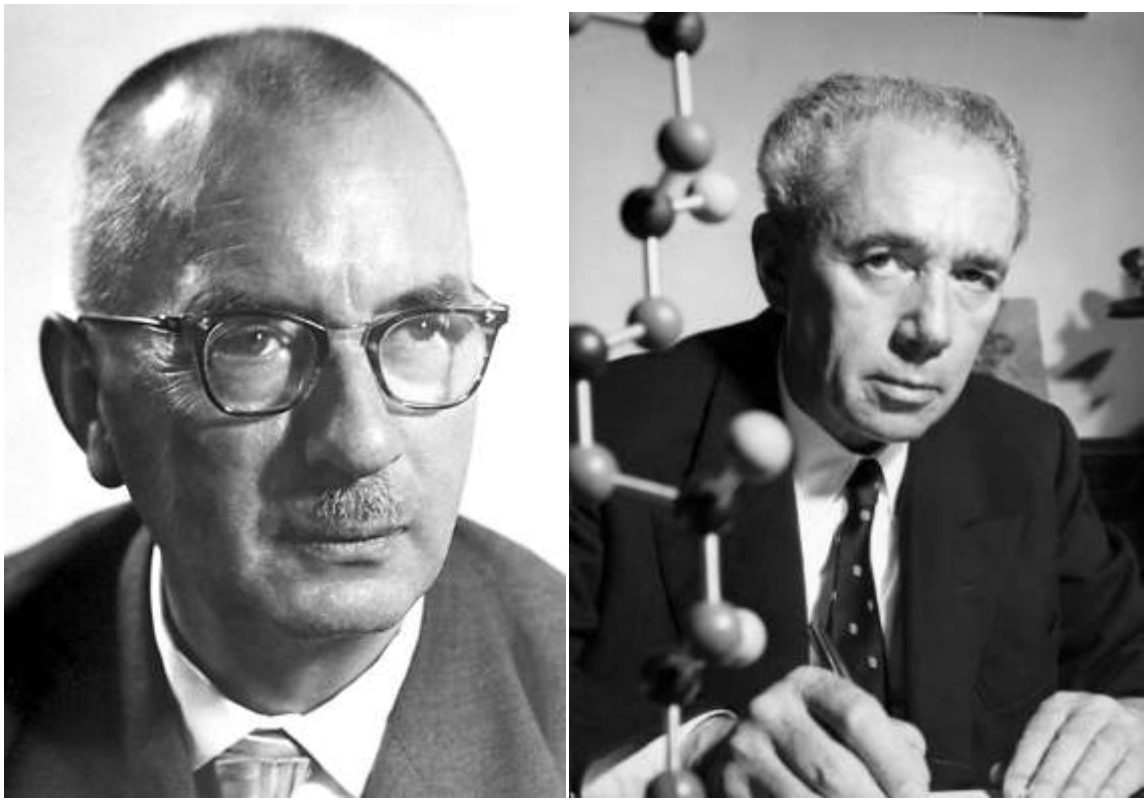


Figure 1.2. Karl Ziegler (left) and Giulio Natta (right) were awarded the Nobel Prize in Chemistry in 1963 for their work with polyolefin catalysts, which are now known as Ziegler-Natta catalysts.[6,8]

Shortly after this discovery, Giulio Natta (Figure 1.2)[8] found that these catalysts were also capable of polymerizing higher α-olefins to give stereoregular polymers, the most industrially important of which is isotactic PP[9] (Figure 1.3) that cannot be made in sufficiently high molecular weight using free radical or ionic polymerization conditions. Isotactic PP is a very tough and semi-crystaline polymer compared to atactic polypropylene that is an amorphous

solid. These heterogeneous catalyst systems are now known as Ziegler-Natta catalysts and unlike free radical or ionic polymerization initiators, the catalyst is not consumed in the polymerization reaction, though they are not recovered in commercial operations due to economic concerns.[5]

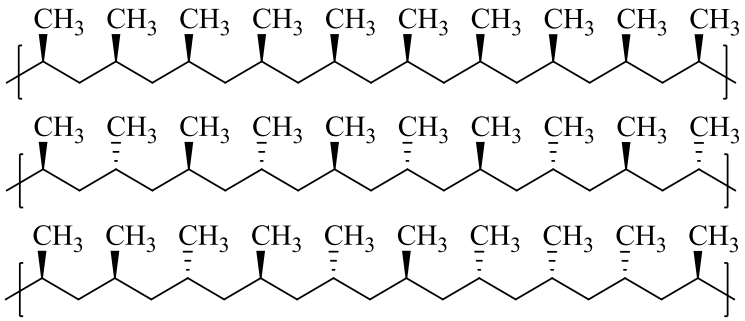


Figure 1.3. Short segments of polypropylene showing the three different types of tacticity: isotactic polypropylene (top), syndiotactic polypropylene (middle), and atactic polypropylene (bottom).

The discovery of these catalysts, which consists of a heterogenous mixture of catalytically active titanium (III or IV) chloride supported on a magnesium chloride matrix (Figure 1.4),[10] has revolutionized the polymer world, providing synthetic access to HDPE and isotactic PP. Figure 1.4 shows how the Titanium atoms on the outer edge of the crystal are not fully coordinated with six other halides, which presents an open site at which an α-olefin may coordinate and polymerize. This feat would eventually win them the Nobel Prize in Chemistry in 1963.[11] Since this discovery, the synthesis of polymers with defined structure and stereochemistry has been a primary focus both in industry and academia. However, owing to

their heterogeneous nature, these catalysts are complex mixtures that have ill-defined structure, have multiple active sites and yield mixtures of polymers with varying properties depending on the polymerization conditions chosen.[1] Because of this, a great amount of research has been directed toward the development of homogeneous, single-site olefin polymerization catalysts.[2]

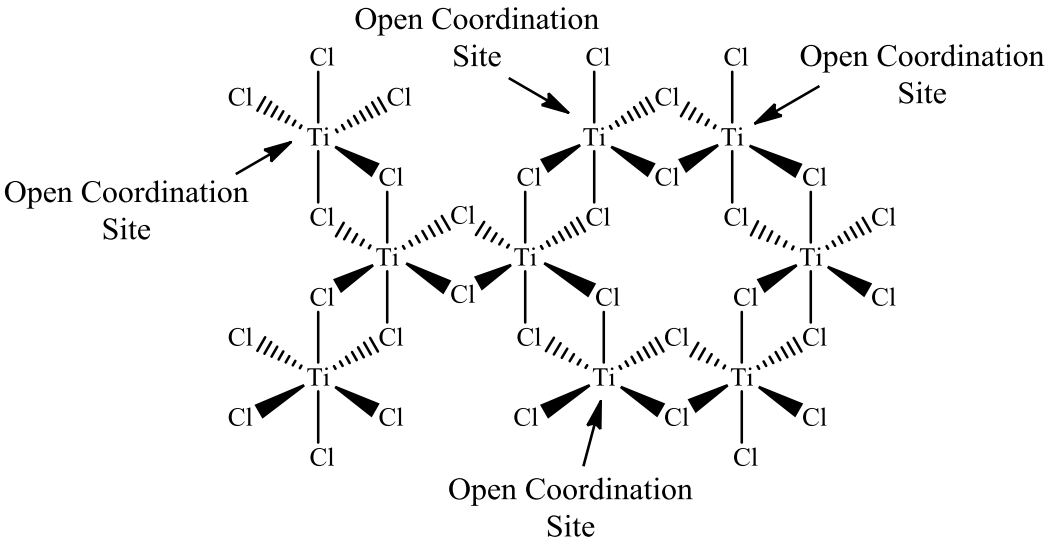
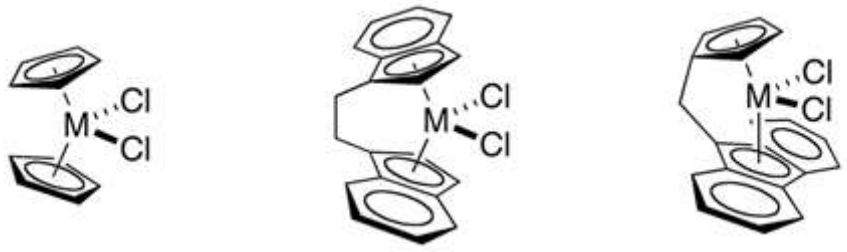


Figure 1.4. A crystal of $TiCl_3$ used in the Ziegler-Natta catalysis of α-olefins.[10]

1.3: Development of Metallocene-Based Olefin Polymerization Catalysts

Shortly after Ziegler and Natta discovered their heterogeneous catalyst systems, Natta and Breslow found that metallocenes such as Cp_2TiCl_2 (Cp = cyclopentadienyl), could be activated with organoaluminums such as triethyl aluminum (Et_3Al) to also polymerize ethylene.[1] These catalysts, which were soluble in organic solvents, polymerized ethylene but failed to polymerize propylene and higher α-olefins. In addition, they demonstrated much lower activities

as compared to their heterogeneous counterparts. Figure 1.5 shows a few examples of metallocene catalysts.[12] Catalyst **1.1** produces atactic polymer, catalyst **1.2** produces isotactic polymer and catalyst **1.3** produces syndiotactic polymer. Though much work was done after the time of this report, very little progress was made toward a well-defined homogeneous system until 1980 when Kaminsky and co-workers discovered that partially hydrolyzed trimethyl aluminum, now called methylaluminoxane (MAO), activated these group 4 metallocenes toward olefin polymerization. Kaminsky's systems were highly active catalysts and were competent for the polymerization of ethylene and propylene as well as higher α-olefins.[13] This discovery led to a paradigm shift in catalyst design with homogeneous, single-site catalysts receiving a tremendous amount of attention in an effort to better understand how these systems functioned.



1.1 **1.2** **1.3**

Figure 1.5. Examples of metallocene catalysts developed by Kaminsky. M = Ti, Zr or Hf.[12]

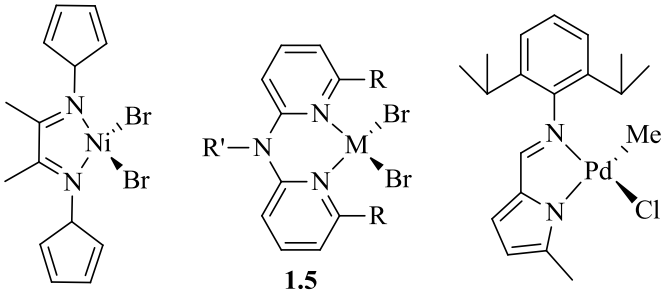
Unlike heterogeneous catalysts, homogeneous systems possess well-defined active sites that have enabled researchers to better understand the mechanistic details of olefin polymerization. This enhanced knowledge has facilitated the development of catalysts that can provide precise control over polymer molecular weight, molecular weight distribution, and

polymer stereochemistry that have lead to a wide range of polymeric materials with new and/or enhanced properties.[14] Metallocene-based catalysts have facilitated the commercial production of high-performance, linear low density PEs (LLDPE), isotactic PP, syndiotactic PP, amorphous copolymers of ethylene/1-butene and many different thermoplastic elastomers. In addition, their development has facilitated the study of the intimate details of the initiation, propagation and termination events of coordination polymerization and stereoselective polymerization, contributing significantly to advances in the catalyst design for controlled olefin polymerization.[2]

1.4: Development of Non-Metallocene Based Olefin Catalysts

Following the discovery of metallocene catalysts, interest soon shifted toward the development of non-metallocene catalysts hoping to harness the potential of numerous other ligand frameworks in the polymerization of olefinic monomers.[15] These frameworks have enabled the fine-tuning of ligand coordination environments and sterics providing easy access to catalysts capable of producing isotactic, syndiotactic and atactic polymers as well as numerous block copolymers. In addition to these non-metallocene catalysts, researchers also discovered highly active catalysts based on group 10 metals, as opposed to group 4, which were capable of polymerizing ethylene to either mostly linear or highly branched PE depending on the metal, ligand and reaction conditions chosen. This demonstrated that it was possible to expand the scope of metals used beyond the first half of the transition series.[16] Since then, numerous metals from group 3 through group 13 have all been used as olefin polymerization catalysts.[15] Figure 1.6 shows three examples of such non-metallocene olefin polymerization catalysts. Catalyst **1.4** is an example of an α-diimine catalyst developed by Brookhart and co-workers while catalyst **1.5** is based off of a class of neutral nitrogen donor ligands. Catalyst **1.6** was developed by Novak

and co-workers and while it is unreactive towards ethylene, **1.6** produces an acrylate rich 1-hexene-methylacrylate copolymer.[2,15]

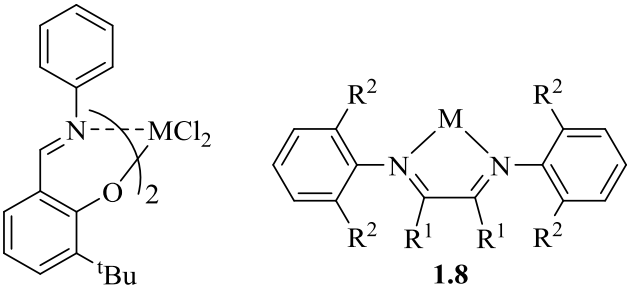


1.4 **1.5** **1.6**

M = Ni, Pd
R = Ph, Me, ^{i}Pr, ^{t}Bu
R' = Ph, Me, ^{i}Pr, ^{t}Bu

Figure 1.6. Examples of non-metallocene catalysts used for olefin polymerization.[2,15]

One area of non-metallocene catalyst research that has received considerable attention are the so called phenoxyimine catalysts developed by Fujita and co-workers[17] (Figure 1.7, catalyst **1.7**) which were developed in the late 1990s. These catalysts, often termed "FI" catalysts, improved upon other phenoxyimine-based systems that had previously shown low activities.[18] When activated, FI catalysts exhibit unprecedented catalytic activity for the polymerization of ethylene.[2] They also found that the activity of the catalyst strongly depended on the nature of the metal and size of the group attached to the imino nitrogen, as well as the substitution in the ortho position of the *N*-aryl group. Their research focused on group 4 metals and found that Zr was the most active followed by Hf, and then Ti.[17]



1.7

M = Ti, Zr, Hf

1.8

M = Ni, Pd
R^1 = H, Me, An
R^2 = H, Me, ^{i}Pr

Figure 1.7. Examples of FI catalysts developed by Fujita, **1.7**, and the α-diimine catalysts developed by Brookhart, **1.8**. An = Acenaphthene.[1,2]

Lastly, another area of non-metallocene catalyst research that has continued to attract much attention are the α-diimine catalysts originally pioneered by Brookhart and co-workers (Figure 1.7, complex **1.8**)[16] Brookhart found that these systems were more tolerant towards contaminants found in solvent and monomer and also permitted the incorporation of monomers containing polar functionality, a feat that was extremely difficult with group 4 metals due to their inherent oxophilicity.[3] Prior to Brookhart's report, known late transition-metal catalysts would typically only oligomerize olefins due to competing β-hydride elimination reactions and associative chain transfer.[16] Brookhart overcame these issues by using bulky ortho substituents on the N-aryl moities, which all but eliminated chain transfer due to monomer coordination at the catalysts axial sites.

1.5: Conclusion

The development of polyolefinic materials has had a profound influence on the world due to their enhanced properties and use in everyday products such as toys packages and bottles. The discovery of Ziegler-Natta catalysts in the 1950s led to the polymerization of ethylene to give HDPE and of higher α-olefins to give stereoregular polymers, the most important being isotactic PP. Although this feat won them the Nobel Prize in Chemistry in 1963, these heterogeneous catalysts have ill-defined active sites leading to mixtures of polymers with varying properties depending on the reaction conditions used. Because of this, a great deal of research has been directed towards the development of homogeneous, single site polymerization catalysts.

Shortly after the discovery of Ziegler-Natta catalysts, Natta and Breslow discovered that homogenous metallocenes could be activated by organoaluminums to also polymerize ethylene. These catalysts were soluble in common organic solvents but failed to polymerize propylene, as well as other higher α-olefins, and displayed lower activities compared to heterogeneous systems. In 1980, Kaminsky found that these group 4 metallocenes could be activated with MAO which led to very active catalysts which polymerized ethylene, propylene and other higher α-olefins. This led to a paradigm shift in catalyst design with homogeneous systems receiving most of the attention. These homogeneous systems possess a well-defined active site which has allowed researchers to better understand how these catalysts work allowing them to design catalysts which lead to a wide range of polymeric material with new and/or enhanced properties.

After the development of metallocene-based catalyst, interest soon shifted towards the development of non-metallocene-based catalyst systems in the hopes of utilizing numerous other

ligand and metal combinations. These systems have led to numerous different atactic, syndiotactic and isotactic polymers as well as different block-copolymers. The discovery of highly active group 10 catalysts demonstrated that it was possible to use many other metals beyond the first half of the transition metals. Lastly, two areas of non-metallocene based catalysts that have received a lot of attention are the FI catalysts developed by Fujita and co-workers and the α-diimine catalysts developed by Brookhart and co-workers, both discovered in the 1990s. The FI catalysts improved upon other group 4 phenoxyimine catalysts with improved performance towards the polymerization of ethylene while it was discovered that the α-diimine catalysts were more tolerant towards contaminants found in solvent and monomer and also allowed the incorporation of monomers which contained polar functionality.

Chapter 2
Redox-Active Olefin Polymerization Catalysts

2.1: Introduction

To date, most post-metallocene catalysts have found little industrial interest for a variety of reasons. First, these catalysts are usually limited in their polymerization scope, such as is the case of group 3 and group 4 catalysts that are known to have poor functional group tolerance. Second, these catalysts often show uncontrolled/non-living polymerization behavior. Lastly, these catalysts frequently have poor activities with higher α-olefin monomers, as is the case with group 10 catalysts.[3] To overcome and/or alleviate many of these downfalls, we plan to incorporate redox-active functionality into our olefin polymerization catalysts. Redox capabilities should allow for the electronic tuning of the active metal site, thereby altering their activity and/or reactivity of those catalysts.

There are many potential advantages of using a redox-active olefin polymerization catalyst. First, the electrophilicity of the propagating metal center may be tuned through the modulation of the ligands electron-donating or electron-withdrawing capabilities that may in turn enhance or retard monomer coordination (Figure 2.1). Second, this change in electronic nature may give rise to monomer selectivity switching that can lead to unique block copolymer structures arising from the oscillation of the catalyst between its reduced and oxidized states. Block copolymers of this nature are known to have unique mechanical properties and have numerous consumer applications such as thermoplastic elastomers.[19] Lastly, switching the

ligand redox-state may lead to an on/off switch in activity creating a reversible dormant/active catalyst system. Likewise, this may also facilitate block copolymer synthesis and/or lead to increased β-hydride elimination and be used as an electrochemical chain transfer agent (CTA) to precisely control/limit molecular weights without adding a separate reagent.[20]

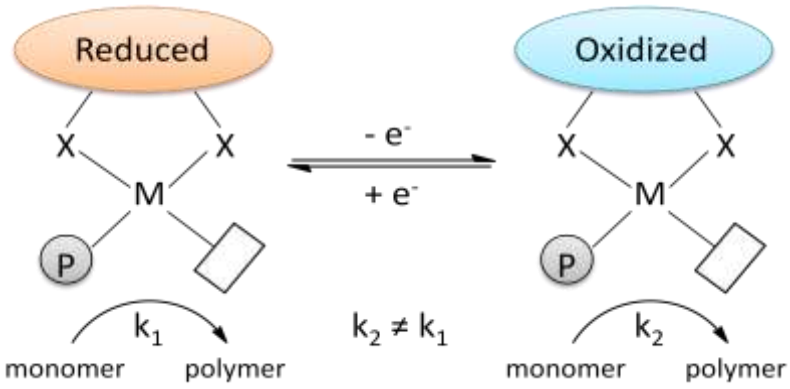


Figure 2.1. Overview of redox-active ligands for olefin polymerization. P = growing polymer chain.

2.2: Previous Research with Redox-Active Catalyst Systems

The ability to regulate or alter the reactivity of a catalyst through the reduction or oxidation of an incorporated redox-active species is a relatively new area of research that has begun to draw a considerable amount of attention in the past years.[21] An initial report by Wrighton in 1995 demonstrated that a diphosphino-cobaltocene stabilized rhodium complex catalyzed the hydrogenation of cyclohexene approximately 16 times faster in the reduced from when compared to the oxidized form of the catalyst (Figure 2.2).[22] Wrighton's initial catalyst was

chemically oxidized *in situ* using Fc^*PF_6 leading to the slow rate of conversion, but could then be chemically reduced via the addition of $CoCp_2$, thereby accelerating the rate of hydrogenation. Similar results were observed with the hydrogenation/isomerization of 1-pentene as well as the transfer hydrogenation of acetone to 2-propanol, which again was faster in the reduced from than that of the oxidized form. This increase in reactivity was attributed to the electron rich Rh center of the reduced form, which was able to facilitate oxidative addition of H_2. In contrast, the oxidized form of the catalyst was faster with the hydrosilation of acetone to isopropoxytriethylsilane and 1-propene to 1-pentyltriethylsilane. [22]

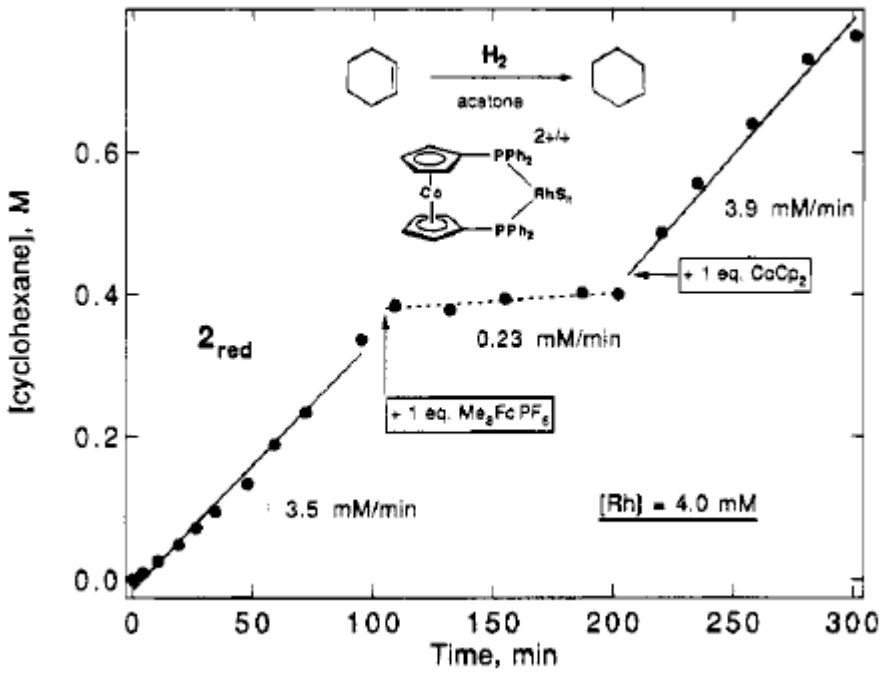
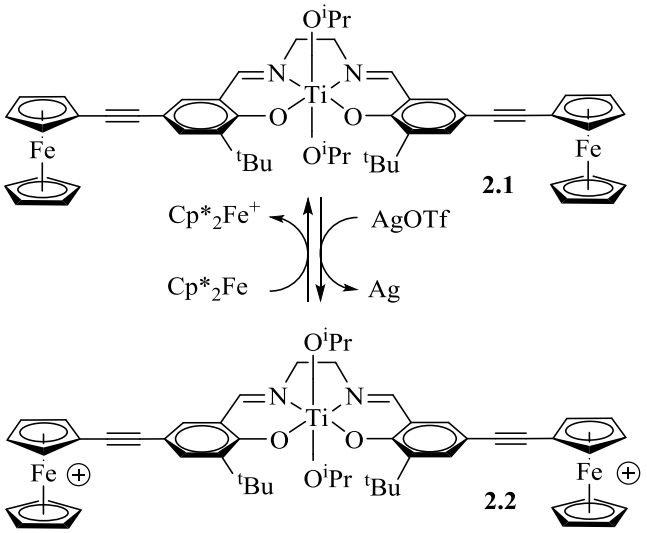


Figure 2.2. A time vs. conversion graph of the hydrogenation of cyclohexene in acetone.[22]

In response to this discovery by Wrighton, the concept of redox-switchable catalysis soon moved to the field of polymer chemistry when in 2006, Gibson and co-workers demonstrated that the activity of a Ti based lactide polymerization catalyst could be varied via redox-switching of a ferrocenyl unit contained within the backbone of the ligand (Scheme 2.1). They proposed that the key to such a ligand is a substantially inert redox-active center. Gibson chose to use a ferrocenyl functionalized bis(iminophenoxide) (salen) titanium catalyst as this class of ligand has been used repeatedly for lactide polymerization catalysis. To identify a suitable chemical oxidant and reductant, the standard half electrode potential of the initial (reduced) ligand was determined, which was found to be 0.08 V (vs Fc/Fc^{+}) (Fc = ferrocene) and hence AgOTf was selected as the chemical oxidant and decamethyferrocene as the chemical reductant. With the addition of AgOTf, the catalyst was oxidized and the polymerization rate slowed substantially, but the polymerization could then be returned back to its initial rate upon addition of decamethyl ferrocene to the polymerization solution, reducing the catalyst (Figure 2.3).[23]

Scheme 2.1: Redox Activity of Gibson's Ti Based Lactide Polymerization Catalyst (**2.1**/**2.2**)[23]



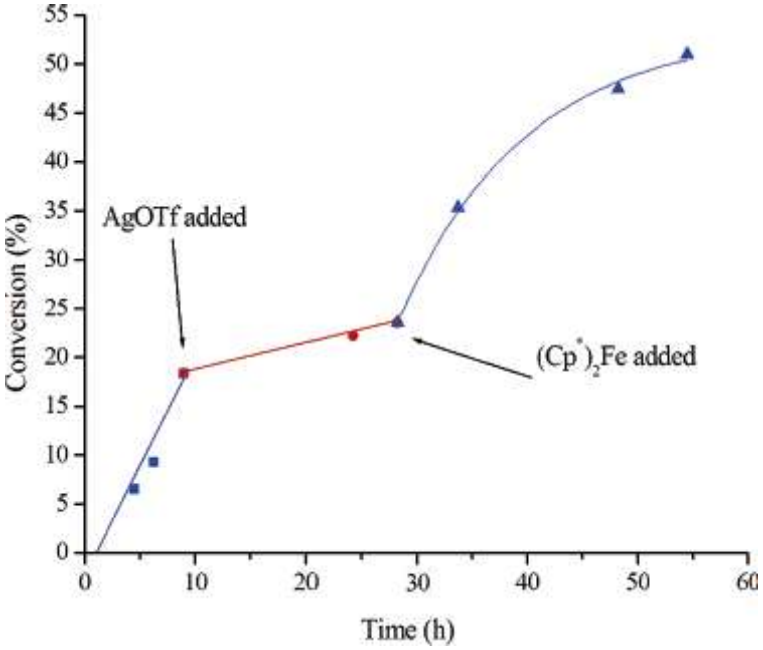
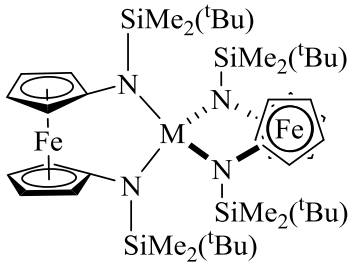


Figure 2.3: A plot of conversion versus time for the polymerization of *rac*-lactide during the in situ oxidation and reduction of complex **2.1**/**2.2** (toluene, 70°C, [LA]0/[Ti]) = 100.[23]

Shortly after Gibson's demonstration of redox-active Ti ligands, Diaconescu and co-workers demonstrated a similar redox potential using uranium and zirconium based complexes in 2007. Again, due to its convenient synthesis and many known derivatives, ferrocenyl-based ligands were used. In this case, 1,1'-disubstituted ferrocene diamides were chosen so that the iron is positioned in close proximity to the metal center.[24] Depending on the distance between the ferrocenyl unit and the metal center, a direct interaction could potentially be observed.[25] They investigated if a direct uranium-iron interaction took place due to the close proximity of the two metal centers, and if so, whether it influenced the reactivity of the uranium center. The complex chosen contained three redox-active metal centers: the two Fe centers of the ferrocene

ligands, which can undergo a Fe(II) to Fe(III) oxidation, and the uranium center, which, theoretically, can undergo a U(IV) to U(V) oxidation (Figure 2.4, complex **2.3**).[24] Along with the U complex, they examined the redox capabilities of an analogous Zr complex and found that both the U and Zr complexes demonstrated significant redox interactions between the U or Zr metal centers and the Fe center of the ferrocenyl units. This demonstrated that the identity of the metal center within a complex plays an important role in how redox activity can be switched in different transition metal complexes.[24]



2.3

M = U, Zr

Figure 2.4. The redox-active metal complex studied by Diaconescu and co-workers.[24]

It should be noted that Gibson and co-workers proposed the use of redox-active olefin polymerization catalysts in 2003 where his work focused on the synthesis and redox potentials of pyridyl-imine ligands with Ni and Pd complexes as olefin polymerization catalysts. In those studies, they found that the ferrocenyl ligands did display redox-activity when examined via cyclic voltammetry (CV), however, when the catalysts were tested for olefin polymerization in

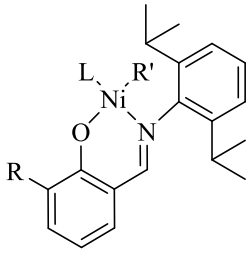
the presence of MAO, the Pd catalysts showed little to no activity and the Ni catalysts only oligomerized ethylene. No high molecular weight PE was produced with either system and no differentiation between redox-states was ever observed.[26] We believe this is due to the use of MAO as a co-catalyst that is known to contain trialkyl aluminum contaminants. Trialkyl aluminums have been shown to reduce ferrocenium derivatives to ferrocene leading to a lack of differentiation between the reduced and oxidized forms. To avoid these issues, we plan to create a redox-switchable olefin polymerization system that does not utilize MAO as an activator. Instead, the use of borate activators may be preferred as they will avoid the possible reduction of ferrocene due to the aluminum contaminants contained in MAO activators.

Our initial efforts have focused on the synthesis of known ligand frameworks where a portion of the ligand has been modified to include a redox-active center. Ferrocene was chosen due to its heavily studied and well understood redox behavior, owing mainly to its reversible electrochemical oxidation from Fe^{II} to Fe^{III} through many different known chemical oxidants. In addition, many derivatives of ferrocene have been reported leading to numerous different starting points for ligand syntheses. Once synthesized, the ligands will be analyzed using CV to determine if they display redox-behavior and whether that behavior is reversible or not. If they do, further studies will be performed to see how they differ in their polymerization capabilities when subjected to different chemical reductants and oxidants.

2.3: Results and Discussion

In analogy to catalysts developed by Grubbs[27] (Figure 2.5, ligand **2.4**) compounds **2.8** and **2.11** (Schemes 2.2 & 2.3) were chosen as initial targets. These catalysts are modified

versions of phenoxyimine ligands that drew significant attention as they could propagate via a neutral Ni^{II} center rather than a traditional cationic metal center without the need for co-catalysts or activators.[28] Since no activator is required, any complications arising catalyst activation can be avoided. However, their utility is often limited as they do not readily polymerize higher α-olefins and only polymerize ethylene slowly when subjected to extremely high monomer pressures. This decreased activity, along with other shortcomings, is attributed to the decreased electrophilic nature of the neutral, salicylaldiminato ligated Ni^{II} center. We believe this activity may be improved with the addition of a redox-active center that may remove electron density from the Ni center, thereby increasing its electrophilicity.

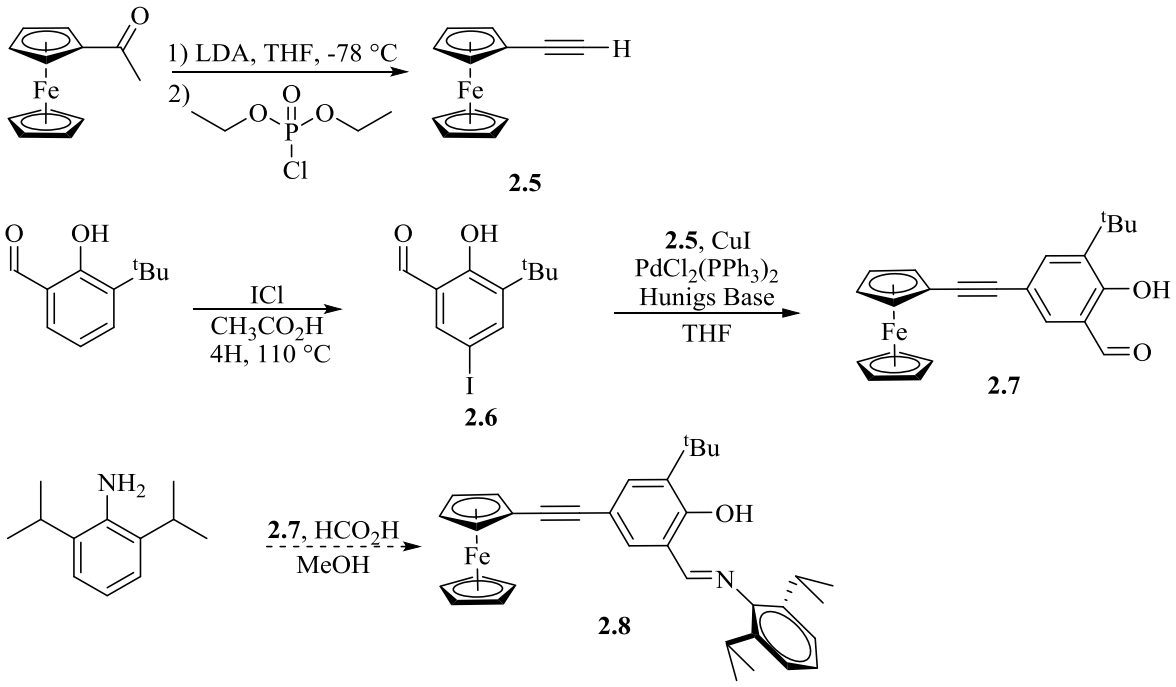


2.4

R = Ph, Phen, Anth,Trityl, TPhen
R' = Ph, CH_3

Figure 2.5. Ni(II) phenoxyimine complex developed by Grubbs. Ph = phenyl, Phen = 9-phenanthroline, Anth = 9-anthracene, Trityl = triphenylmethyl, Tphen = *meta*-terphenyl.[27]

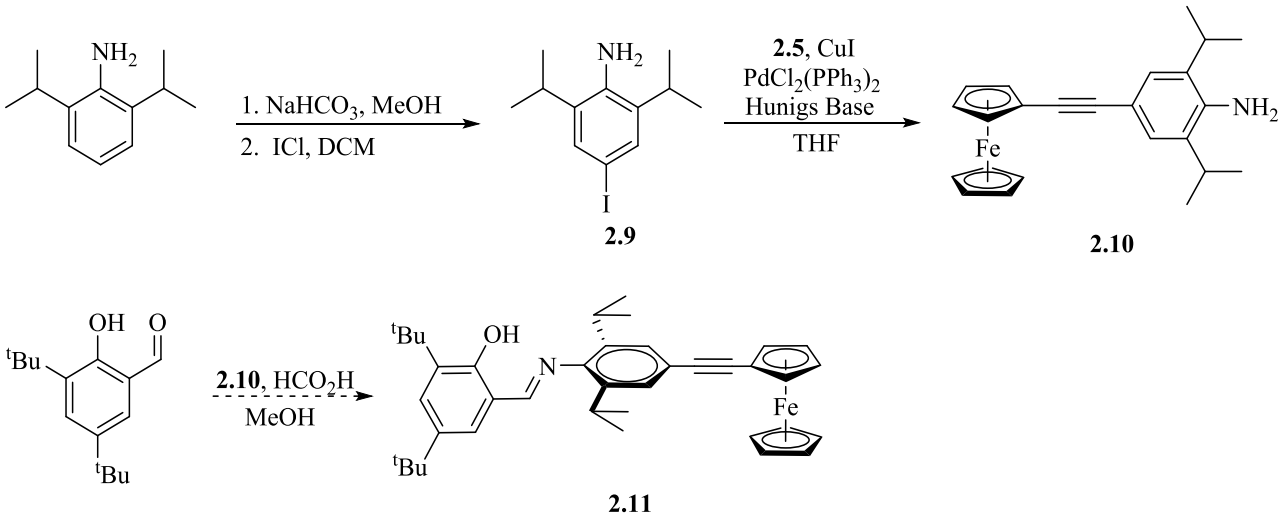
Scheme 2.2 Synthesis of ethynylferrocene phenoxyimine ligand **2.8**



Compound **2.8** (Scheme 2.2) was synthesized via Sonogashira coupling of ethynylferrocene,[29] **2.5**, with 3-tert-butyl-5-iodosalicyladehyde,[30] **2.6**, followed by imine condensation with commercially available 2,6-diisopropylaniline. Compound **2.11** (Scheme 2.3) was synthesized in a similar manner with the location of the ferrocene moiety being changed. Compound **2.10** was synthesized via Sonogashira coupling of ethynylferrocene, **2.5**, with 4-iodo-2,6-diisopropylaniline,[31] **2.9**, and then condensed onto commercially available 3,5-di-tert-butyl-2-hydroxybenzaldehyde via imine formation. Although both ligands are similar in structure, the location of the redox-active ferrocenyl moiety may play an important role in how the catalyst behaves when subjected to different redox and polymerization conditions. In the future, a

catalyst with a ferrocenyl center in both locations may also be of interest to see if further catalyst modulation can be observed with two redox-active centers as compared to one.

Scheme 2.3 Synthesis of ethynylferrocene phenoxyimine ligand **2.11**

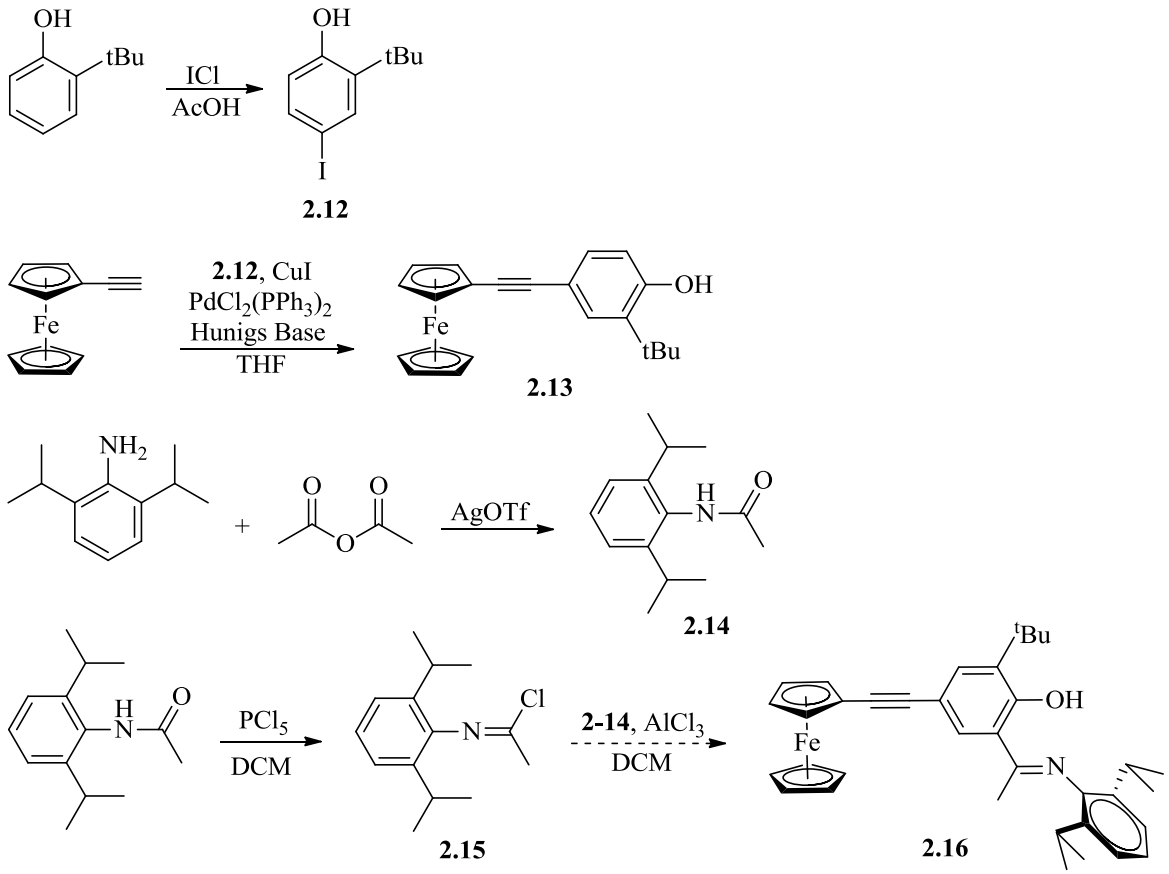


Currently, we are in the process of optimizing the reaction conditions that produce both ligands **2.8** and **2.11**. We have observed in the condensation of sterically hindered anilines, such as 2,6-diisopropylaniline onto salicylaldehyde **2.7**, that mixtures are obtained and that significant amounts of starting material remain. We speculate that this could be attributed to the increase electron density present in the π system due to ferrocene's electron donating capability. We are currently examining methods in which this reaction can be driven to the desired product as separation of residual starting material has proven difficult via recrystalization or column chromatography. Likewise, similar results have been observed in the synthesis of phenoxyimine **2.11** in which starting material is present under the conditions examined. Purification in this

case succumbs to the above mentioned difficulties, and we are also looking for alternative means to drive this reaction to products.

Due to the difficulties encountered with synthesizing ligands **2.8** and **2.11**, a new ligand was chosen. This new target is a phenoxyketimine catalyst, **2.13,** (Scheme 2.4) that was chosen because it is derived from imine formation at a ketone rather than the more common aldehyde. This ketimine should be more stable as they are known to be less prone to hydrolysis. This enhanced stability should allow for purification via column chromatography whereas most imines are not stable to typical chromatographic seperations due to their ease of hydrolysis.

Scheme 2.4: Synthesis of phenoxyketimine **2.16**.

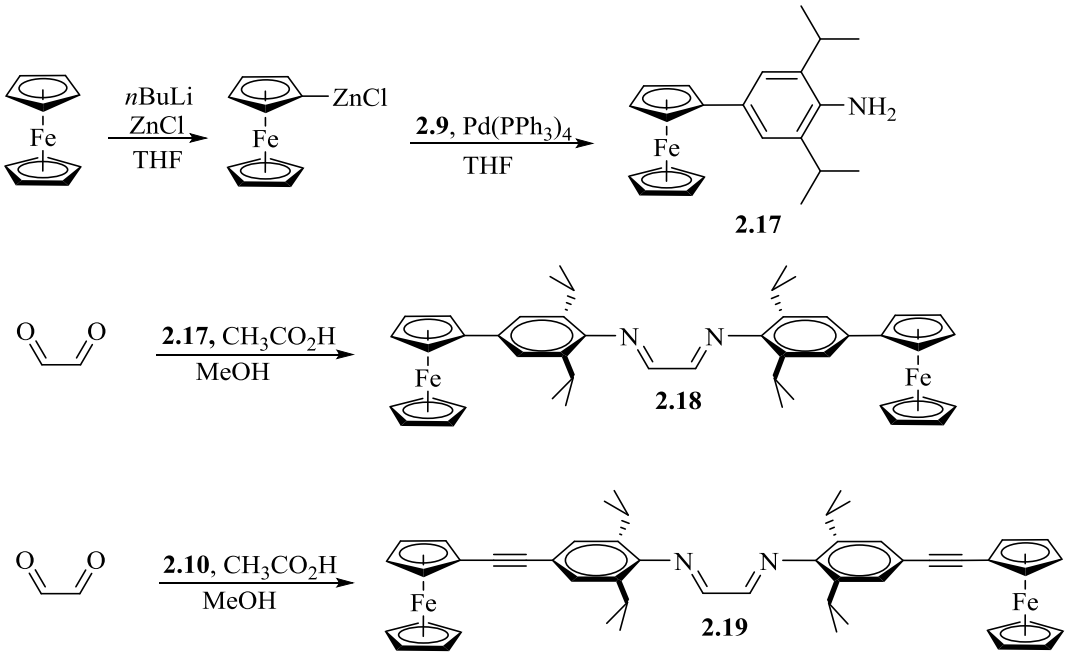


Compound **2.13** was synthesized via Sonogashira coupling of phenol **2.12**[32] with ethynylferrocene, **2.5** (Scheme 2.4). Ligand **2.16** was then synthesized via Friedel-Crafts acylation of phenol **2.13** with imidoyl chloride **2.15** that was formed in situ by reacting acetamide **2.14**[33] with PCl_5 (Scheme 2.5)**.** NMR analysis shows formation of the ligand, however, purification of the ligand has been difficult via crystallization and column chromatography due to a complex mixture of products. We believe this is because the Friedel-Crafts reaction requires an activated ring in order for the reaction to occur. However, compound **2.16** has more than one activated ring for the reaction to occur so we believe the imidoyl chloride, **2.15**, is adding onto the phenol ring as well as the cyclopentadienyl ring of ferrocene. This has led to a mixture of products that have been difficult to separate.

In order to avoid the synthetic pitfalls encountered above, we decided to focus our efforts on the synthesis of α-diimine-based catalysts. Group 10 catalysts utilizing this framework have been studied, but have found little industrial use for a variety of reasons including having low activities with many different types of monomers. Probing the redox-activity of these catalysts may present us with a chance to electrochemically reduce the catalysts and allow us to see if this reduced state has an effect on the polymerization characteristics of the catalysts. Ligands **2.18** and **2.19** (Scheme 3.6) are both modified versions of Brookhart-type α-diimine ligands where the N-aryl moieties have been modified with ferrocenyl groups. Ultimately, we want to coordinate these α-diimine ligands with different Pd sources. This is because the Pd catalysts do not need to be activated with MAO as they already can be synthesized with a metal alkyl bond that will facilitate coordination and insertion of olefinic monomers. This will eliminate the reduction of ferrocenium normally associated with the use of MAO. Aniline **2.17**[34] condensed quite easily

onto glyoxal to give α-diimine **2.18**. Ligand **2.19** was synthesized in a similar fashion to give α-diimine **2.19** where an ethynyl-bridge separates the N-aryl group from the redox active ferrocene moiety.

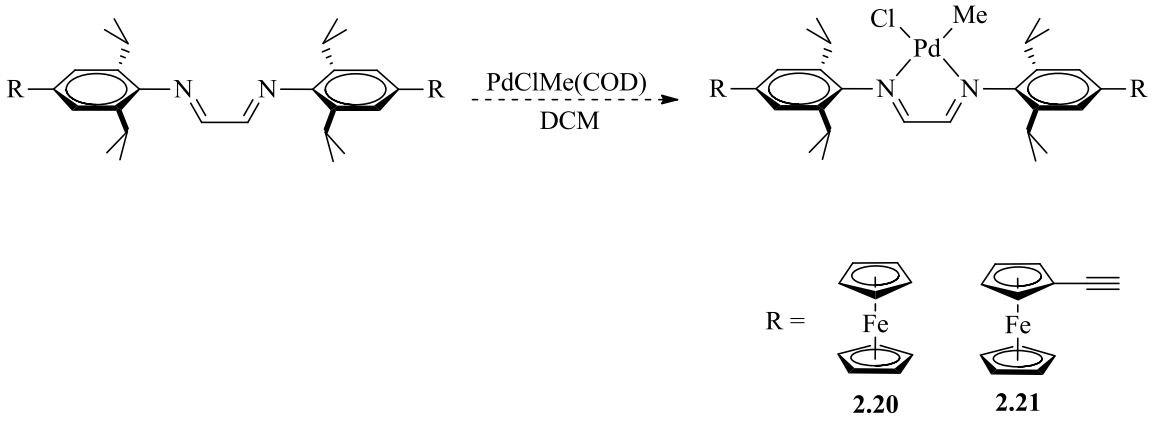
Scheme 2.5: Synthesis of α-diimine ligands **2.18** and **2.19.**



After completing the synthesis of ligands **2.18** and **2.19**, the coordination of ligand **2.19** with PdClMe(COD) to give complexes **2.21** was attempted (Scheme 2.7). To date, this has only been done on a small scale to confirm that coordination would occur. Almost immediately, the solution changed color from yellow to brown, however, the ^{1}HNMR did not show evidence that coordination occurred when proton shifts of the free ligand were compared to the complex. After further examination, it was found that the DCM used during coordination contained a

substantial amount of water. This may have resulted in the poisoning of the palladium complex used prior to coordination. Currently, the coordination is being explored using dry DCM.

Scheme 2.6: Synthesis of palladium complexes **2.20** and **2.21**.

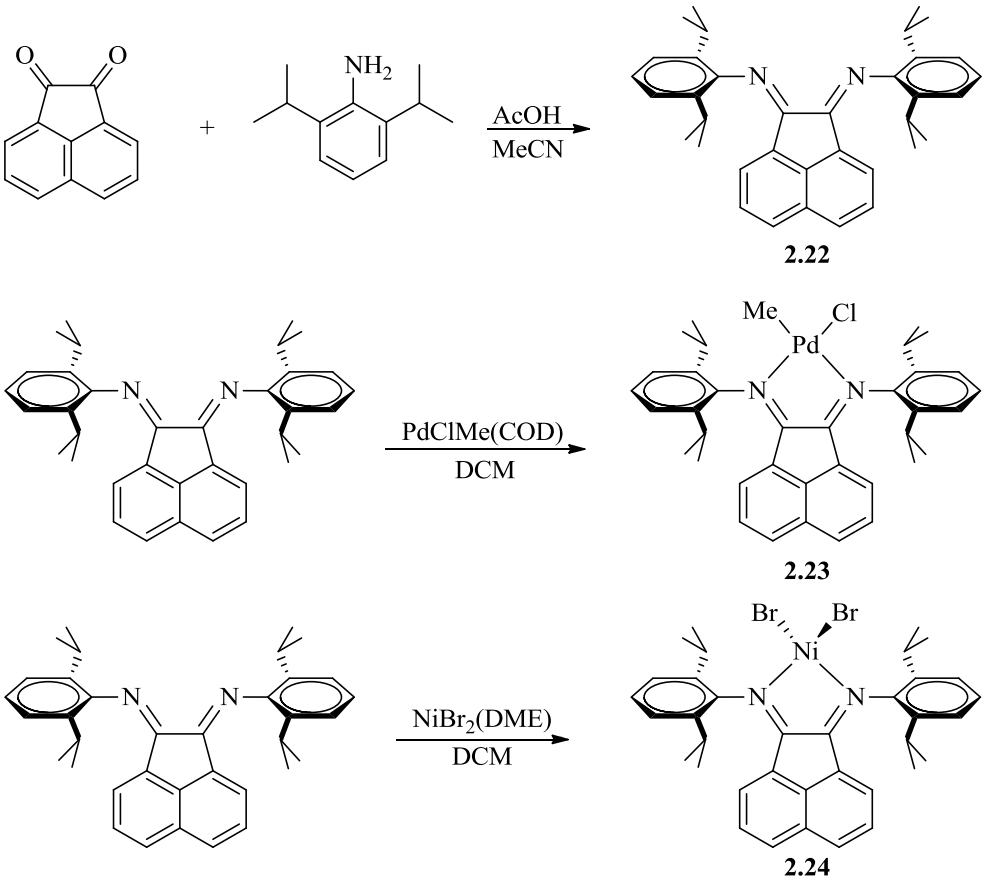


To date, the coordination of ligand **2.18** with PdClMe(COD) has not been attempted. This is because initially, only a small amount of ligand **2.18** was synthesized for characterization and work has focused on the synthesis and coordination of ligand **2.19**. It is believed though that ligand **2.18** will coordinate in a similar fashion compared to the coordination of **2.19**.

After the synthesis of ligands **2.18** and **2.19**, it was thought that the ferrocenyl substituted anilines would condense readily onto commercially available acenaphthenequinone but this was found not to be the case. We believe that this is due to the fast electron transfer of the easily oxidized ferrocene and the quickly reduced acenaphthenequinone, preventing the imine condensation reaction. Because of this, a question was proposed as to whether the

acenaphthenequinone based Brookhart ligands could exhibit redox activity without any added redox active moieties.[35] Because of this, the Brookhart type ligands were synthesized. The α-diimine **2.22**[36] (Scheme 2.7) was synthesized via imine condensation of commercially available acenaphthenequinone with commercially available 2,6-diisopropylaniline in the presence of acetic acid as a catalysts to give the Bis(aryl)acenaphthenequinonediimine (aryl = 2,6-diisopropylaniline) (BIAN) ligand, **2.22**. The resulting α-diimine was then coordinated with PdClMe(COD)[37] and $NiBr_2$(DME) to give complexes **2.23** and **2.24** (Scheme 2.7) respectively.

Scheme 2.7: Synthesis of α-diimine ligand **2.22** and complexes **2.23** and **2.24**



2.4: Redox-Activity of Catalysts and Polymerizations

The redox-activity of each ligand was explored using cyclic voltammetry (CV). As Figure 2.6 shows, the PdClMe(BIAN) catalyst shows a reduction at -1.48 V and an oxidation at -1.33 V relative to a ferrocene standard. This allowed us to use cobaltacene as a suitable chemical reducing agent which has a reduction potential of -1.33 V versus ferrocene.[38] Catalysts **2.23** was reduced in situ prior to use with the addition of 1 equivalent of cobaltacene to give the reduced catalyst **2.25** (Scheme 2.8). The catalyst was reduced before being activated so only the reduced version of the catalyst was activated as opposed to the original oxidized catalyst being activated.

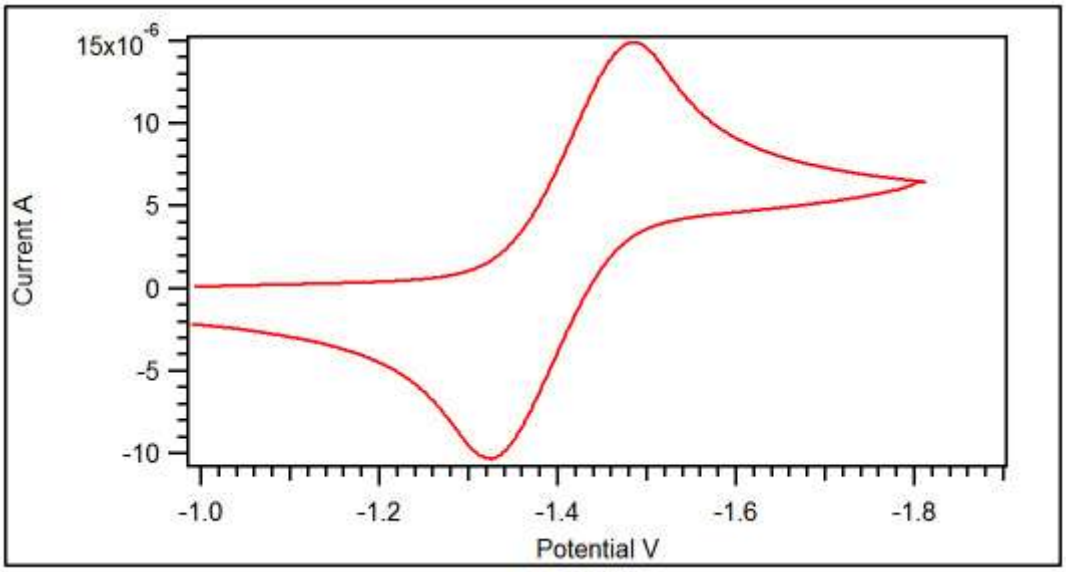
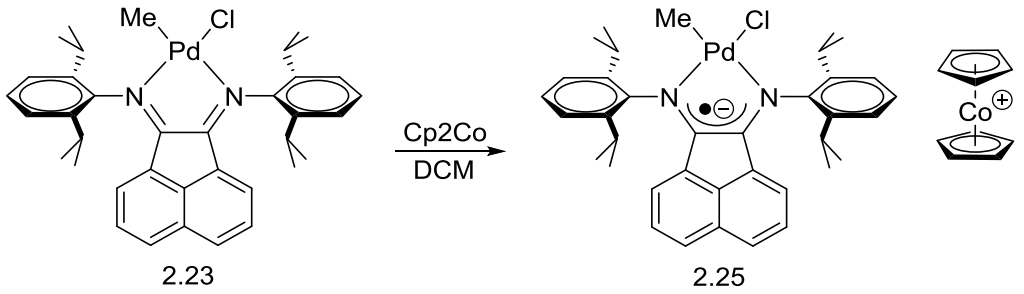


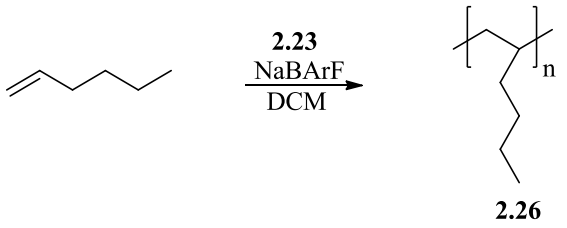
Figure 2.6. Cyclic voltammetry curve for the PdClMe(BIAN) catalyst corrected to ferrocene. The curve shows a reduction at -1.48 V and an oxidation at -1.33 V with a half-wave potential of -1.41 V.

Scheme 2.8: The reduction of PdClMe(BIAN), **2.23**, using Cp_2Co to give catalyst **2.25**.



Initial polymerizations were ran for 24 hours in order to record molecular weights and polydispersity indexes (PDI) via gel permeation chromatography (GPC). The polymerization of 1-hexene was achieved by using PdClMe(BIAN) as a catalyst and sodium tetrakis[3,5-bis(trifluoromethyl)phenyl]borate (NaBArF) as an activator in dichloromethane (DCM). The reaction was then quenched with acidic methanol (5 % HCl in MeOH) to give polymer **2.26** (Scheme 2.8). The monomer of choice for these reactions was 1-hexene due to its quick availability and the fact that it is a liquid at room temperature making it much easier to handle when compared to gaseous monomers such as ethylene and propylene.

Scheme 2.9: The Polymerization of 1-hexene using the PdClMe(BIAN) to give polymer **2.26**.



Initially, a polymerization of 1-hexene with PdClMe(BIAN) in toluene was ran as stated above using polymethylaluminoxane-improved performance (PMAO) as an activator instead of NaBArF to give polymer **2.26** as well**.** MAO is typically used as an activator since polymerizations require an open coordination site and a metal-alkyl bond for the polymerization to initiate and propagate. However, the palladium precursor we used already has a metal-alkyl bond avoiding the need for MAO, but this did allow us to see whether MAO or NaBArF was a better activator choice for this polymerization. Using PMAO as an activator gave a very small amount of polymer (2.60 mg) over the 48 hour polymerization run. GPC samples were then prepared by dissolving 5.00 mg of polymer in 5.00 mL of THF. The samples were ran using THF as a mobile phase and referenced to polystyrene standards giving a number average molecular weight (M_n) of 14.00 kg/mol and a weight average molecular weight (M_w) of 18.00 kg/mol, and a PDI of 1.30 (Figure 2.6). Due to the small amount of polymer obtained using PMAO as an activator, all future polymerization using PdClMe(BIAN) as a catalyst were ran using NaBArF as the activator.

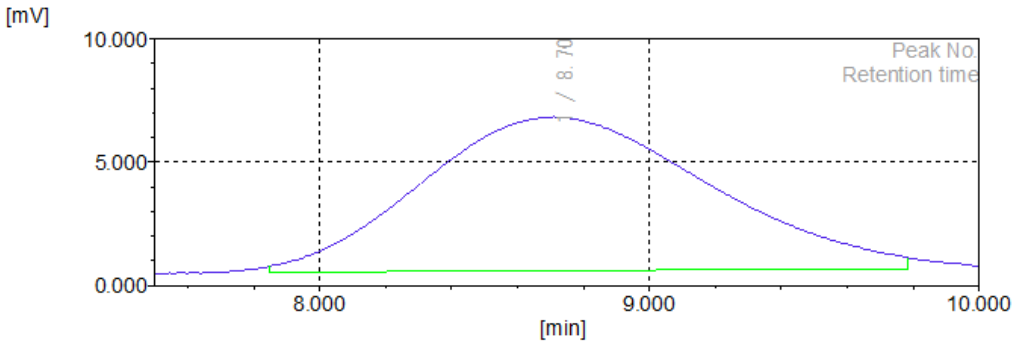


Figure 2.7: GPC analysis of poly-1-hexene using PdClMe(BIAN) as a catalyst and PMAO as an activator.

Using NaBArF as an activator, the polymerization of 1-hexene over 24 hours gave a very viscous polymer (773.5 mg). GPC analysis gave a M_n of 13.00 kg/mol, a M_w of 19.00 kg/mol and a PDI of 1.46 (Figure 2.7). The PDI was larger than the PDI of the polymer made using PMAO, but the amount of polymer made would allow better kinetic experiments to be conducted.

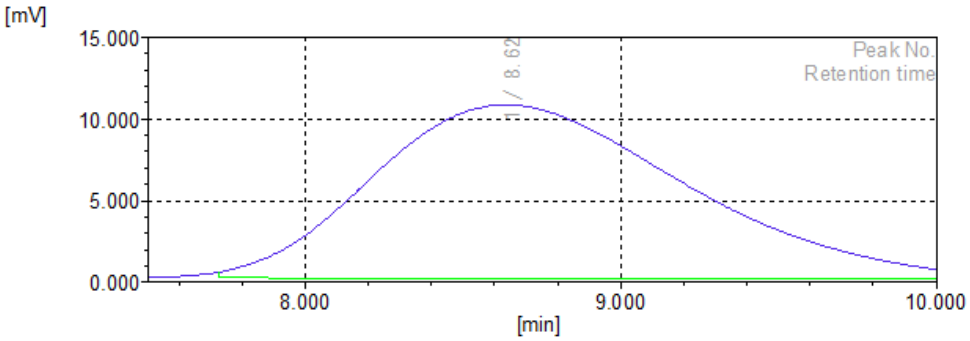


Figure 2.8: GPC analysis of poly-1-hexene using PdClMe(BIAN) as a catalyst and NaBArf as an activator.

Following this, polymerization kinetics were measured by running a similar, larger scale polymerization in which 1 mL aliquots of the solutions were removed and quenched with acidic MeOH to measure the percent conversion at certain time points (Table 2.1). Three trials were ran in order to calculate the average percent conversion at each time point as well as to calculate the standard deviation between each of the trials.

Table 2.1: Data showing the mass of polymer obtained and percent conversion of all three trials ran in the polymerization of polymer **2.26**.

	Trial 1		Trial 2		Trial 3	
Time (min.)	**Polymer (mg)**	**Conversion (%)**	**Polymer (mg)**	**Conversion (%)**	**Polymer (mg)**	**Conversion (%)**
5	3.60	11.15	1.10	3.41	3.10	9.60
10	5.60	17.35	2.50	7.74	3.00	9.29
15	6.70	20.76	2.10	6.51	4.40	13.63
25	6.90	21.38	4.00	12.39	5.50	17.04
45	12.50	38.72	5.20	16.11	8.00	24.78
60	13.70	42.44	7.20	22.30	8.50	26.33
90	14.30	44.30	9.80	30.36	11.70	36.25
120	17.60	54.52	12.60	39.03	13.70	42.44
180	22.90	70.94	15.40	47.71	17.30	53.59
240	26.70	82.71	19.60	60.72	20.80	64.44
300	32.20	99.75	20.00	61.96	22.40	69.39
360	31.00	96.03	20.70	64.13	20.60	63.82
1440	25.00	77.45	23.40	72.49	22.50	69.70
2880	27.20	84.26	22.10	68.46	22.80	70.63

As Table 2.1 shows, the polymerization reaches maximum conversion in approximately 300 min, which can also be seen in Figure 2.9. This gives an average peak conversion rate just above 70 %. We believe that the palladium catalyst decomposes over this time leading to the low conversion rate. Currently, different reaction conditions, such as using a different solvent or lower temperature, are being explored in order to try to get the reaction to reach 100 % conversion.

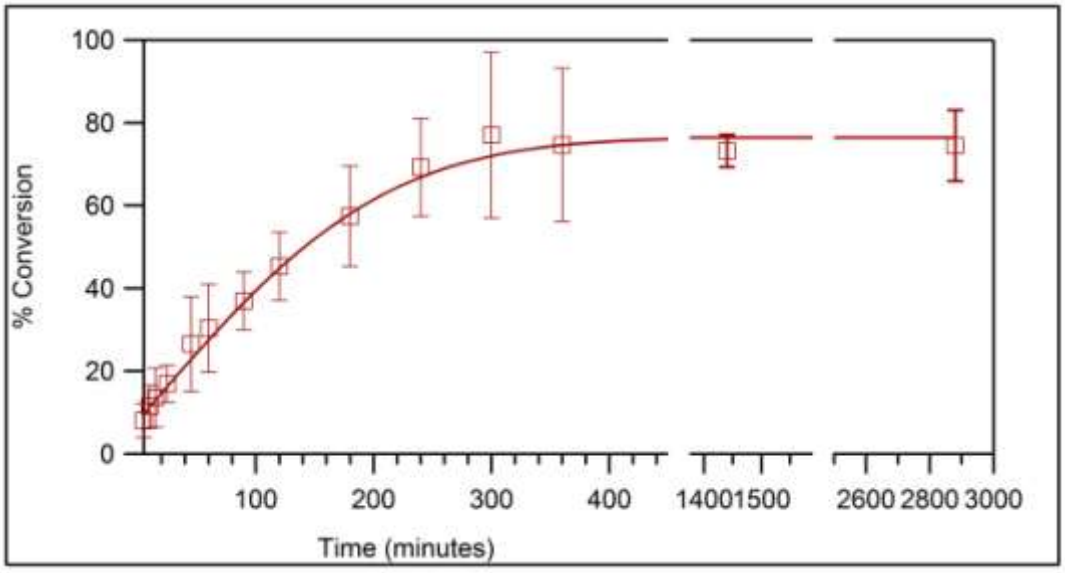
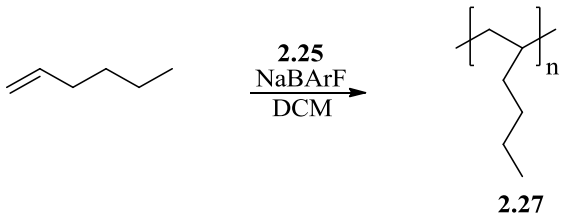


Figure 2.9. A percent conversion versus time graph for the polymerization of 1-hexene using PdClMe(BIAN) as a catalyst and NaBArF as activator

After all initial polymerizations were done, a set of polymerizations were ran with the addition of cobaltacene which acts as a chemical reductant in order to reduce the catalyst to see if the reduced version polymerized at a different rate compared to the initial oxidized catalysts. Cobaltacene was added to the catalyst prior to being activated so only the fully reduced version of the catalyst, **2.25**, would be activated for the polymerization of 1-hexene to give polymer **2.28** (Scheme 2.10).

Scheme 2.10: The polymerization of 1-hexene using the reduced PdClMe(BIAN) catalyst to give polymer **2.27**.



2.27

After activation, 1 mL aliquots were taken to measure percent conversion at the given time points so the percent conversion at each time could be compared to the conversion rate of the original, non-reduced catalyst (Table 2.2). Like the original polymerizations, three trials were again measured in order to give a time versus conversion graph for the polymerization of polymer **2.27** (Figure 2.10).

Table 2.2: Data showing the amount of polymer obtained and percent conversion of all three trials ran in the polymerization of polymer **2.27**.

	Trial 1		Trial 2		Trial 3	
Time (min.)	**Polymer (mg)**	**Conversion (%)**	**Polymer (mg)**	**Conversion (%)**	**Polymer (mg)**	**Conversion (%)**
5	0.30	0.93	0.10	0.31	0.10	0.31
10	0.60	1.86	0.10	0.31	0.10	0.31
15	0.90	2.79	0.40	1.24	0.70	2.17
25	0.90	2.79	1.20	3.72	2.30	7.13
45	2.90	8.98	1.50	4.65	3.70	11.46
60	2.30	7.13	4.50	13.94	5.60	17.35
90	4.20	13.01	5.90	18.28	7.80	24.16
120	5.10	15.80	6.10	18.90	8.40	26.02
180	6.10	18.90	7.00	21.69	9.70	30.05
240	7.00	21.69	7.80	24.16	9.60	29.74
300	6.60	20.45	7.80	24.16	9.80	30.36
360	5.60	17.35	8.10	25.09	10.00	30.98
1440	6.70	20.76	7.70	23.85	8.30	25.71
2880	6.50	20.14	5.50	17.04	3.60	11.15

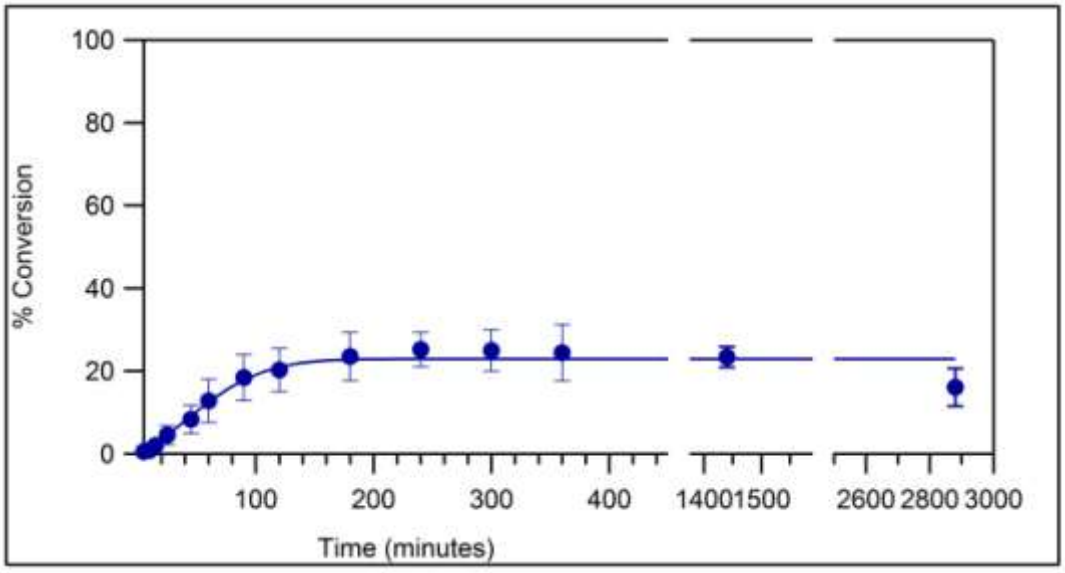


Figure 2.10. A percent conversion versus time graph for the polymerization of 1-hexene using the reduced PdClMe(BIAN) catalyst and NaBArF as activator.

As Figure 2.10 shows, the reduced catalyst results in a much slower conversion rate when compared to the original non-reduced catalyst. Along with that, the highest percent conversion achieved is just over 20 % compared to 70 % with the original, non-reduced catalyst. Again, we believe this is due to the decomposition of the palladium catalyst. Figure 2.11 shows the reduced and oxidized catalyst conversion rate. A polymerization was also ran under the exact same conditions, but it was allowed to polymerize for two weeks in order to see if the polymerization ever reached 100 %. Unfortunately, after two weeks, the percent conversion was still just over 20 %.

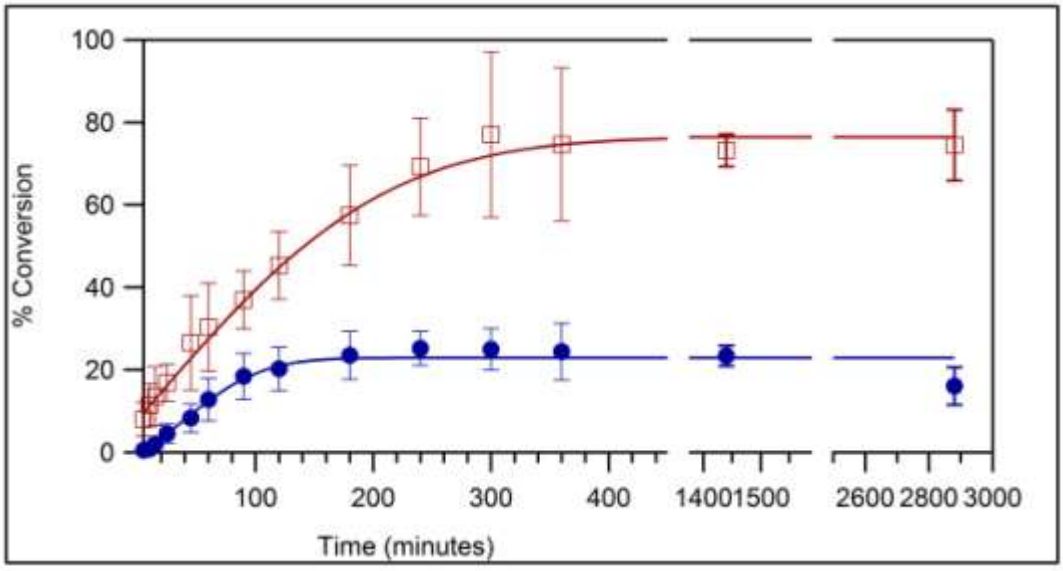


Figure 2.11. A time versus percent conversion graph for the polymerization of 1-hexene showing the reduced and oxidized PdClMe(BIAN) catalyst. Both catalysts were activated using NaBArF.

A post-doctoral associate in our group ran a similar experiment using a nickel based catalyst instead of the palladium based catalyst. The polymerization of 1-hexene to give polymer **2.28** using $NiBr_2$(BIAN) as a catalyst was reacted in toluene using PMAO as an activator instead of NaBArF (Scheme 2.11). This is because the nickel catalyst used does not have the necessary metal-alkyl bond needed to initiate polymerization without PMAO. The kinetics of the polymerization were also measured in the same way as they were measured using the palladium based catalyst. As Figure 2.12 shows, the polymerization of 1-hexene reached 100 % conversion for both the original and reduced forms of the $NiBr_2$(AIBN) catalyst.

Scheme 2.11: The polymerization of 1-hexene using the $NiBr_2$(BIAN)to give polymer **2.28.**



2.28

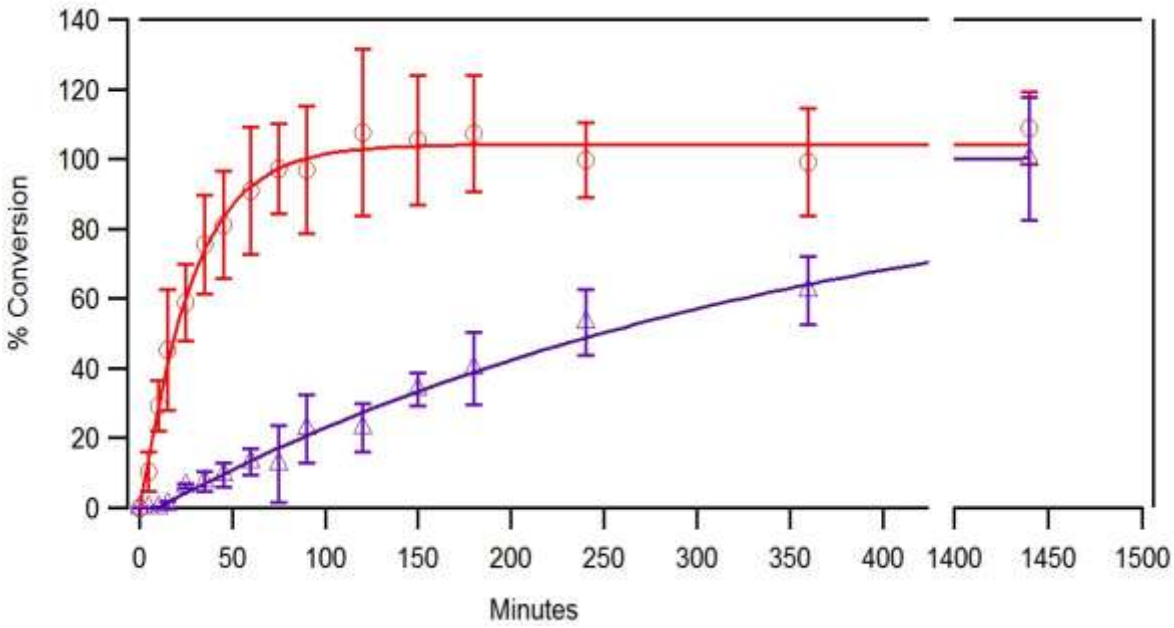


Figure 2.12. A percent conversion versus time graph for the polymerization of 1-hexene using $NiBr_2$(BIAN) as a catalyst and PMAO as an activator. The graph shows the different polymerization rates between the original, non-reduced catalyst (red line) and the reduced catalyst (purple line). Both polymerizations reached 100 % conversion over the 48 hour period.

2.5: Conclusion

Presented are three different phenoxyimine and phenoxyketimine ligands as well as two different α-diimine based ligands that contain ferrocene as a potential redox-active center. Difficulties were encountered with the synthesis of the phenoxyimine and phenoxyketimine ligands with their purification being elusive to date. Glyoxal-based α-diimine ligands were synthesized due to difficulties encountered with the imine condensation of acenapthenequinone to give α-diimine ligands **2.18** and **2.19**. Currently, ligand **2.19** is in the process of being coordinated with PdClMe(COD) with the coordination of ligand **2.18** to follow. Finally, the

original Brookhart based ligand **2.22** was synthesized and coordinated with PdClMe(COD) and $NiBr_2$(DME) to give complexes **2.23** and **2.24** respectively. These complexes were found to be redox-active via CV and their polymerization attributes are currently being explored in both their oxidized and reduced states for the polymerization of 1-hexene.

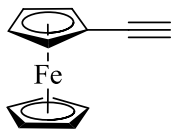
Initially, the kinetics of both catalytic systems were explored over a 48 hour period in order to see how the original catalyst polymerized 1-hexene into polyhexene. The nickel based catalyst was successful in reaching 100 % conversion while the palladium catalyst was only successful in reaching just over 70 % conversion. This is being attributed to the possible decomposition of the palladium catalyst and different reaction conditions are currently being explored in order to reach 100 % conversion with the palladium catalyst.

Following this, the redox-activity of each catalyst was explored by chemically reducing each catalyst in situ with cobaltacene before activation occurred. Again, the kinetics of each polymerization were explored over 48 hours in order to see if the polymerization rate of the reduced catalyst was different compared to the original, non-reduced catalyst. It was found that the reduced catalyst does polymerize at a slower rate for both the Ni and Pd-based catalyst systems when compared to the oxidized catalysts. Here, the nickel catalyst did reached 100 % conversion over extended reactions due to the slower propagation of the reduced catalyst, but the palladium catalyst only reached 25 % conversion.

Experimental Section

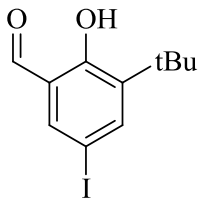
General Remarks: All air and moisture sensitive reactions were performed under an inert atmosphere of nitrogen using standard Schlenk or glove box techniques. All solvents were dried via standard solvent purification techniques and degassed via freeze, pump, thaw cycles (3x each). All reagents and solvents were purchased from Acros Organics, Fisher Scientific, Sigma-Aldrich or synthesized via literature methods. NMR analysis was done using either a Varian Mercury Vx 300 MHz or Varian VNMRS 500 MHz and referenced to standard solvents. Mass spectromety analysis was completed done using a JEOL AccuTOF™ DART Mass Spectrometer. GPC analysis were ran using a Tosoh EcoSEC GPC System and polystyrene standards.

Synthesis of Ethynylferrocene (2.5)



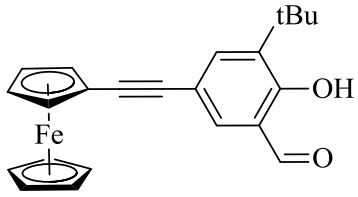
Acetylferrocene (5.0 g, 21.92 mmol) and THF (50 mL) were added to a Schlenk flask and cooled to -78 °C before LDA (1.1 eq, 2.0 M in THF/Heptane/Ethylbenzene) was added dropwise. The mixture was stirred for 1 hour and then diethylchlorophophate (3.98 g, 23.06 mmol) was added dropwise and stirred for an additional 1 hour. The reaction was warmed to room temperature and stirred for 30 minutes before recooling to -78 °C and adding 2.3 additional equivalents of LDA solution. Stirring was continued for an additional hour. The mixture was warmed to room temperature and hydrolized at 0 °C. The organic layer was separated and the aqueous layer was extracted with hexanes (3x100 mL). The combined organic layers were washed with water (2 x 50 mL) and brine (2 x 50 mL), dried with $MgSO_4$ and solvent removed under vacuum to give a crude orange oil. The crude product was purified via column chromatography (5:95 ethyl acetate:hexanes, $R_f = 0.60$) to give dark orange crystals (3.13 g, 68%). All characterization matched the literature.[29]

Synthesis of 3-t-butyl-5-iodo-2-hydroxybenzaldehyde (2.6)



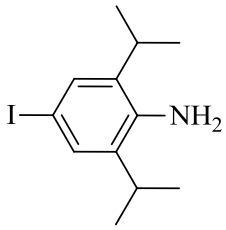
3-t-butyl-2-hydroxybenzaldehyde (1.63 g, 9.14 mmol) was dissolved in acetic acid (10 mL) and stirred for 5 minutes. A solution of iodine monochloride (2.26 g, 13.9 mmol) in acetic acid (15 mL) was added dropwise over 30 minutes before being refluxed for 4 hours. Water (100 mL) was added and stirred for an additional 10 minutes. The mixture was extracted with dichloromethane (3 x 50 mL) and the combined organic layers were washed with a saturated sodium thiosulfate solution, dried with $MgSO_4$ and solvent removed under vacuum to give crude 3-t-butyl-5-iodo-2-hydroxybenzaldehyde. The crude mixture was purified by column chromatography (5:95 ether:pentane, $R_f = 0.61$) to give a pale yellow solid (2.78 g, 83%). All characterization matched the literature.[30]

Synthesis of 3-t-butyl-5-ethynylferrocene-2-hydroxybenzaldehyde (2.7)



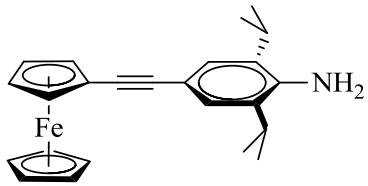
Copper odide (0.031 g, 0.165 mmol) and $PdCl_2(PPh_3)_2$ (0.462 g, 0.658 mmol) were added to an oven dried Schlenk flask. A degassed mixture of ethynylferrocene (1.52 g, 7.23 mmol) and 3-t-butyl-5-iodo-2-hydroxybenzaldehyde (2.0 g, 6.58 mmol) in THF (10 mL) was stirred for 5 minutes, then added via cannula to a flask containing copper iodide and $PdCl_2(PPh_3)_2$ and stirred for 5 minutes. Diisopropylethylamine (1.7 g, 13.16 mmol) was added and the mixture was stirred at 55 °C for 15 hours. The solvent was removed under vacuum and the product was purified by column chromatography (10:90, dichloromethane:hexanes, $R_f = 0.14$) to give orange crystals (2.0 g, 78%). All characterization matched the literature.[23]

Synthesis of 4-iodo-2,6-diisopropylaniline (2.9)



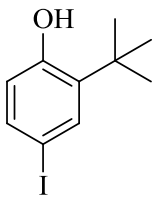
2,6-diisopropylaniline (10.0 g, 56.0 mmol) and sodium bicarbonate (14.2 g, 169.0 mmol) in methanol (80 mL) was stirred for 10 minutes. Iodine monochloride (10.1 g, 62.0 mmol) in dichlorometthane (60 mL) was added drop wise over 1 hour. The mixture was stirred for 20 hours, filtered through a pad of celite, washed with methanol and solvent removed via rotary evaporation. Saturated sodium thiosulfate solution (300 mL) was added and the mixture was stirred for 30 minutes, extracted with ether (3 x 100 mL) and concentrated under vacuum to give a dark red oil (15.76 g, 92%). All characterization matched the literature. [31]

Synthesis of 4-ethynylferrocene-2,6-diisopropylaniline (2.10)



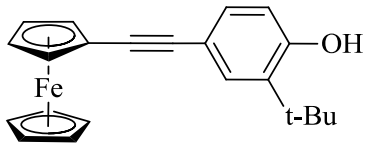
Copper iodide (0.062 g, 0.325 mmol) and $PdCl_2(PPh_3)_2$ (0.912 g, 1.299 mmol) were added to an oven dried Schlenk flask. A degassed solution of ethynylferrocene (3.0 g, 14.29 mmol) and 4-iodo-2,6-diisopropylaniline (3.94 g, 12.99 mmol) in THF (10 mL) was stirred for 5 minutes before being added via cannula to the reaction flask containing copper iodide and $PdCl_2(PPh_3)_2$. This flask was stirred for 5 minutes and then diisopropylethylamine (3.36 g, 25.98 mmol) was added and stirred at 55 °C for 15 hours. The mixture was filtered through a pad of celite, washed with THF and solvent removed under vacuum. The crude product was purified via column chromatography (10:90, ethylacetate:hexanes, R_f = 0.31) to give a dark orange/red oil (1.00 g, 46%). All characterization matched the literature.[34]

Synthesis of 4-iodo-2-tert-butylphenol (2.12)



2-tert-butylphenol (4.04 g, 27.20 mmol) was dissolved in acetic acid (40 mL). A solution of iodine monochloride (4.4 g, 27.20 mmol) in acetic acid (20 mL) was added drop wise and refluxed for 4 hours. The reaction was cooled to room temperature and stirred overnight before being poured into water (300 mL) and extracted with dichloromethane (3 x 100 mL). The combined organic layers were washed with aqueous sodium thiosulfate (3 x 25 mL), water (3 x 25 mL), dried with $MgSO_4$ and then the solvent removed. The crude product was purified via column chromatography (10:90 ethylacetate:hexanes, R_f = 0.24) to give a yellow oil (4.72 g, 64%). All characterization matched the literature.[32]

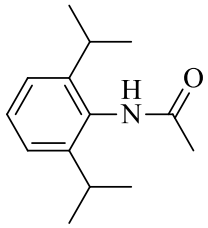
Synthesis of 4-ethynylferrocene-2-tert-butylphenol (2.13)



A degassed solution of Ethynylferrocene (4.00 g, 19.05 mmol) and 4-iodo-2-tert-butylphenol (5.25 g, 19.05 mmol) in triethylamine (100 mL) was stirred for 5 minutes before being added via cannula to an oven dried Schlenk flask containing copper Iodide (0.29 g, 1.52 mmol) and $PdCl_2(PPh_3)_2$ (1.07 g, 1.52 mmol) and stirred at 55 °C for 15 hours. The solution was cooled to room temperature, filtered through celite and washed with triethylamine. The filtrate was then poured into a mixture of dichloromethane and NH_4Cl (2M). The organic layer was separated and the aqueous layer was extracted with dichloromethane (3 x 100 mL), dried with $MgSO_4$ and solvent removed under vacuum. The crude orange powder was purified via trituration in triethylamine followed by a hot filtration. The product then precipitated in triethylamine to give an orange powder (4.19 g, 62%). ^{1}H-NMR (300 MHz, $CDCl_3$) δ: 1.41(s, 9H), 4.21 (t, J = 1.8 Hz, 2H), 4.24 (s, 5H), 4.48 (t, J = 1.8 Hz, 2H), 6.60 (d, J = 8.1 Hz, 1H), 7.21 (dd, J = 8.1, 2.1 Hz,

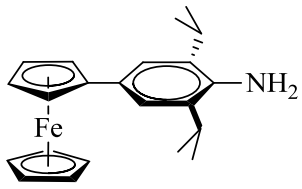
1H), 7.39 (d, J = 2.0 Hz, 1H). ^{13}C NMR (125 MHz, $CDCl_3$) δ: 29.59, 34.79, 45.92, 66.26, 68.65, 70.04, 71.38, 85.78, 115.13, 116.78, 130.39, 130.69, 136.77, 155.22. DART-MS (M +1 359.11 m/z).

Synthesis of N-(2,6-diisopropylphenyl)acetamide (2.14)



Acetic anhydride (4.32 g, 42.30 mmol) was added to an oven dried Schlenk flask containing 2,6-diisopropylaniline (5.0 g, 28.20 mmol) and AgOTf (72.0 mg, 0.282 mmol). The solution stirred at 60 °C for 30 minutes before being quenched with a saturated $NaHCO_3$ solution. The organic layer was separated and the aqueous layer was extracted with ethyl acetate (3 x 50 mL). The combined organic layers were dried with $MgSO_4$ and the solvent removed under vacuum to give white crystals (5.01 g, 81%). All characterization matched the literature.[33]

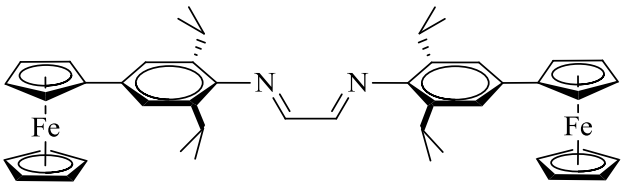
Synthesis of 4-ferrocenyl-2,6-diisopropylaniline (2.17)



Ferrocene (1.30 g, 7.00 mmol) was dissolved in THF (50mL) and then cooled to -20 °C. A solution of n-BuLi (11.00 mL, 1.6 M in Hexanes) was added dropwise then warmed to room temperature and stirred for an additional 30 minutes. The solvent was removed via vacuum and the residue was re-dissolved in THF (30 mL). A solution of anhydrous $ZnCl_2$ (0.95 g, 7.00 mmol) in THF (10 mL) was added and the mixture stirred for 30 minutes before being added to a solution of $Pd(PPh_3)_4$ (0.100 g, 0.087 mmol) and 4-iodo-2,6-diisopropylaniline (1.73 g, 5.70 mmol) in THF (30 mL). The solution stirred for 16 hours at room temperature, refluxed for 1 hour, quenched with a 0.1 M HCl solution (50 mL) and extracted with $CHCl_3$ (3 x 20 mL). The combined organic layers were washed with water and brine, then dried with $MgSO_4$ and concentrated under vacuum. The

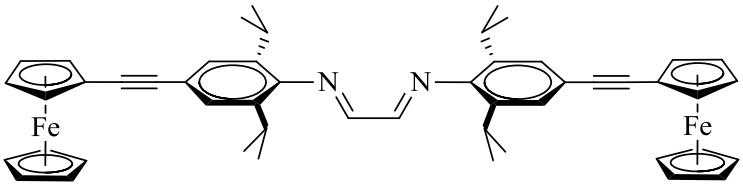
crude product was purified via column chromatography (10:90, ethylacetate:hexanes, R_f = 0.28) to give an orange oil (0.57 g, 28%). All characterization matched the literature.[34]

Synthesis of N,N'-(ethane-1,2-diylidene)bis(4-ferrocenyl-2,6-diisopropylaniline) (2.18)



To a solution of 4-ferrocenyl-2,6-diisoproplyaniline (0.57 g, 1.59 mmol) in MeOH (10 mL) was added 5 drops of acetic acid. Glyoxal (0.09g, 0.80 mmol) was added and the mixture was stirred overnight at 55 °C overnight. A precipitate formed that was isolated via filtration, washed with cold MeOH and dried under vacuum to give a dark orange solid (0.12 g, 21%). ^{1}H-NMR (500 MHz, $CDCl_3$) δ: 1.27 (d, J = 6.9 Hz, 18 H), 3.00 (p, J = 6.9 Hz, 4 H), 4.08 (s, 10 H), 4.31 (t, J = 1.8 Hz, 4 H), 4.62 (t, J = 1.8 Hz, 4 H) 7.30 (s, 4 H), 8.15 (s, 2 H). ^{13}C-NMR (125 MHz, $CDCl_3$) δ: 23.68, 28.17, 66.87, 68.70, 69.67, 87.00, 121.69, 135.89, 136.90, 146.38, 163.22.

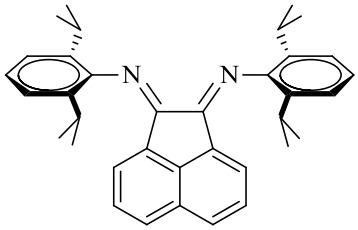
Synthesis of N,N'-(ethane-1,2-diylidene)bis(4-ferrocenyl-2,6-diisopropylaniline (2.19)



To a solution of 4-ethynyl ferrocene-2,6-diisopropylaniline (0.60 g, 1.56 mmol) in MeOH (10 mL) was added 5 drops of acetic acid. Glyoxal (0.045 g, 0.78 mmol) was added and the mixture was stirred overnight at 55 °C overnight. A precipitate formed that was isolated via filtration, washed with cold MeOH and dried under vacuum to give a yellow solid (0.23 g, 38 %). ^{1}H-NMR (500 MHz, $CDCl_3$) δ: 1.23 (d, J = 6.9 Hz, 24 H), 2.93 (m, J = 6.9 Hz, 4 H), 4.25 (t, J = 1.9 Hz, 4 H), 4.27 (s, 10 H), 4.52 (t, J = 1.8 Hz, 4 H) 7.31 (s, 4 H), 8.08 (s, 2 H). ^{13}C-NMR (125 MHz,

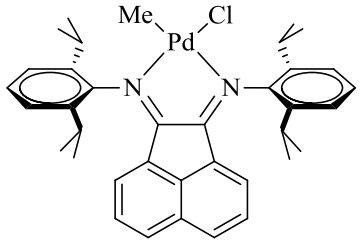
$CDCl_3$) δ: 23.43, 28.20, 65.76, 68.88, 70.10, 71.52, 86.43, 87.22, 120.67, 126.74, 137.19, 147.81, 163.08.

Synthesis of N,N'-(acenaphthylene-1,2-diylidene)bis(2,6-diisopropylaniline) (BIAN) (2.22)



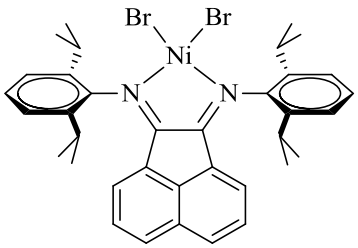
A solution of acenaphthenequinone (7.00 g, 38.40 mmol) and acetonitrile (150 mL) was refluxed for 60 minutes. Acetic acid (65 mL) was added and stirring continued until all of the acenaphthenequinone dissolved. 2,6-diisopropylaniline (13.95 g, 78.82 mmol) was added drop wise over 30 minutes and the solution refluxed for 5 hours before cooling to room temperature. A precipitate formed that was isolated via filtration, washed with pentane (2 x 20 mL) and dried under vacuum to a bright yellow/orange powder. (17.5 g, 91 %) All characterization matched the literature.[36]

Synthesis of PdClMe(BIAN) (2.23)



$PdCl_2$(COD) (0.26 g, 0.99 mmol), N,N'-(acenaphthylene-1,2-diylidene)bis(2,6-diisopropylaniline) (0.50 g, 0.99 mmol) and dichloromethane (30 mL) were added to an oven dried Schlenk flask and stirred for 20 hours. The solution was filtered through celite, washed with dichloromethane (2 x 5 mL) and solvent removed under vacuum. The crude dark orange product was washed with ether (2 x 10 mL) to give a dark orange powder (0.57 g, 87%). All characterization matched the literature.[39]

Synthesis of $NiBr_2$(BIAN) (2.24)



$NiBr_2$(DME) (0.50 g, 1.62 mmol), N,N'-(acenaphthylene-1,2-diylidene)bis(2,6-diisopropylaniline) (0.85 g, 1.70 mmol) and dichloromethane (30 mL) were added to an oven dried Schlenk flask and stirred for 20 hours. The solution was filtered through celite, washed with dichloromethane (2 x 5 mL) and solvent removed under vacuum. The crude red product was washed with ether (2 x 10 mL) to give a dark red powder (0.60 g, 83%). All characterization matched the literature.[16]

Polymerizations

Polymerization of 1-hexene by PdClMe(BIAN)/NaBArF. (2.26) To a flask was added PdClMe(BIAN) (6.53 mg, 10 µmol), NaBARF (10.6 mg, 1.2 eq.) and dichloromethane (8 mL). The solution was stirred for 5 minutes before 1-hexene (2 mL) was added. The solution was stirred for 24 hours before being quenched with a 5% HCl/MeOH solution (30 mL) to give a grey/brown polymer (773.5 mg), M_n = 13.00 kg/mol, M_w = 19.00 kg/mol, PDI = 1.46.

Polymerization of 1-hexene by PdClMe(BIAN)/PMAO. To a flask was added PdClMe(BIAN) (6.53 mg, 10 µmol), 1-hexene (2 mL) and toluene (8 mL) which was stirred while PMAO (0.430 mL, 100 eq) was added. The solution was stirred for 24 hours before being quenched with a 5% HCl/MeOH solution (30 mL) to give a grey/brown polymer (2.6 mg), M_n = 14.00 kg/mol, M_w = 18.00 kg/mol, PDI = 1.30.

Polymerization Kinetics

General Procedure: To a flask was added PdClMe(BIAN) (10 μmol, 6.53 mg) and DCM (20 mL). The solution was added to a flask containing NaBArf (10.6 mg, 1.2 eq.) and stirred for 5 minutes before 1-hexene (1 mL, 8.06 mmol) was added and 1mL aliquots were removed and quenched with acetic methanol (10 mL) (5% HCl/MeOH) at the following time points: 5 min., 10 min., 15 min., 25 min., 45 min., 1 hour, 1.5 hours, 2 hours, 3 hours, 4 hours, 5 hours, 6 hours, 24 hours and 48 hours. The polymers were dried under vacuum overnight at 75 °C.

Polymerization of 1-hexene with PdClMe(BIAn) (reduced) (2.27). The polymerization was ran according to the general procedure except Cobaltacene (1.89 mg, 1 eq) was added to the flask containing PdClMe(BIAn) before being activated with NaBArF.

References

1. Coates, G. W., *Chem Rev*. **2000,** *100*, 1223-1252.
2. Makio, H.; Terao, H.; Iwashita, A.; Fujita, T., *Chem Rev.* **2011,** *111*, 2363-2449.
3. Ittel, S. D.; Johnson, L. K.; Brookhart, M., *Chem Rev.* **2000,** *100*, 1169-1203.
4. Annual report of the American Chemical Council, **2011**.
5. Stevens, M. P., *Polymer chemistry : an introduction*, 3rd ed.; Oxford University Press: New York, 1999.
6. See wikipedia, *Karl Ziegler*, http://en.wikipedia.org/wiki/Karl_Ziegler.
7. Ziegler, K.; Holzkamp, E.; Breil, H.; Martin, H., *Angew Chem Int Edit.* **1955,** *67*, 541-547.
8. See *Giulio Natta: padre della plastica*, http://leganerd.com/2011/01/12/giulio-natta-il-padre-della-plastica/.
9. Natta, C., *J Polym Sci.* **1960,** *48*, 219-239.
10. See *Ziegler-Natta Vinyl Polymerization*, http://www.pslc.ws/macrog/ziegler.htm.
11. Galli, P.; Vecellio, G., *Prog Polym Sci.* **2001,** *26*, 1287-1336.
12. See Wikipedia, *Kaminsky catalyst*, http://en.wikipedia.org/wiki/Kaminsky_catalyst.
13. Sinn, H.; Kaminsky, W.; Vollmer, H. J.; Woldt, R., *Angewandte Chemie-International Edition in English.* **1980,** *19*, 390-392.
14. Brintzinger, H. H.; Fischer, D.; Mulhaupt, R.; Rieger, B.; Waymouth, R. M., *Angewandte Chemie-International Edition in English.* **1995,** *34*, 1143-1170.
15. Gibson, V. C.; Spitzmesser, S. K., *Chem Rev.* **2003,** *103*, 283-315.
16. Johnson, L. K.; Killian, C. M.; Brookhart, M., *J Am Chem Soc.* **1995,** *117*, 6414-6415.
17. Matsui, S.; Fujita, T., *Catal Today.* **2001,** *66*, 63-73.

18. Cozzi, P. G.; Gallo, E.; Floriani, C.; Chiesivilla, A.; Rizzoli, C., *Organometallics.* **1995,** *14*, 4994-4996.

19. Hotta, A.; Cochran, E.; Ruokolainen, J.; Khanna, V.; Fredrickson, G. H.; Kramer, E. J.; Shin, Y. W.; Shimizu, F.; Cherian, A. E.; Hustad, P. D.; Rose, J. M.; Coates, G. W., *P Natl Acad Sci USA.* **2006,** *103*, 15327-15332.

20. Hustad, P. D.; Kuhlman, R. L.; Carnahan, E. M.; Wenzel, T. T.; Arriola, D. J., *Macromolecules.* **2008,** *41*, 4081-4089.

21. Allgeier, A. M.; Mirkin, C. A., *Angew Chem Int Edit.* **1998,** *37*, 894-908.

22. Lorkovic, I. M.; Duff, R. R.; Wrighton, M. S., *J Am Chem Soc.* **1995,** *117*, 3617-3618.

23. Gregson, C. K. A.; Gibson, V. C.; Long, N. J.; Marshall, E. L.; Oxford, P. J.; White, A. J. P., *J Am Chem Soc.* **2006,** *128*, 7410-7411.

24. Monreal, M. J.; Carver, C. T.; Diaconescu, P. L., *Inorg Chem.* **2007,** *46*, 7226-7228.

25. Akabori, S.; Kumagai, T.; Shirahige, T.; Sato, S.; Kawazoe, K.; Tamura, C.; Sato, M., *Organometallics.* **1987,** *6*, 2105-2109.

26. Gibson, V. C.; Halliwell, C. M.; Long, N. J.; Oxford, P. J.; Smith, A. M.; White, A. J. P.; Williams, D. J., *Dalton T.* **2003**, 918-926.

27. Wang, C. M.; Friedrich, S.; Younkin, T. R.; Li, R. T.; Grubbs, R. H.; Bansleben, D. A.; Day, M. W., *Organometallics.* **1998,** *17*, 3149-3151.

28. Younkin, T. R.; Conner, E. F.; Henderson, J. I.; Friedrich, S. K.; Grubbs, R. H.; Bansleben, D. A., *Science.* **2000,** *287*, 460-462.

29. Doisneau, G.; Balavoine, G.; Fillebeenkhan, T., *J Organomet Chem.* **1992,** *425*, 113-117.

30. Nielsen, M.; Gothelf, K. V., *J Chem Soc Perk T 1.* **2001**, 2440-2444.

31. D'Souza, B. R.; Lane, T. K.; Louie, J., *Org Lett.* **2011,** *13*, 2936-2939.

32. Bombis, C.; Weigelt, S.; Knudsen, M. M.; Norgaard, M.; Busse, C.; Laegsgaard, E.; Besenbacher, F.; Gothelf, K. V.; Linderoth, T. R., *Acs Nano.* **2010,** *4*, 297-311.

33. Das, R.; Chakraborty, D., *Synthesis-Stuttgart.* **2011**, 1621-1625.

34. Siemeling, U.; Neumann, B.; Stammler, H. G.; Kuhnert, O., *Polyhedron.* **1999,** *18*, 1815-1819.

35. Baker, R. J.; Farley, R. D.; Jones, C.; Mills, D. P.; Kloth, M.; Murphy, D. M., *Chem-Eur J.* **2005,** *11*, 2972-2982.

36. Dastgir, S.; Coleman, K. S.; Cowley, A. R.; Green, M. L. H., *Organometallics.* **2010,** *29*, 4858-4870.

37. Rulke, R. E.; Ernsting, J. M.; Spek, A. L.; Elsevier, C. J.; Vanleeuwen, P. W. N. M.; Vrieze, K., *Inorg Chem.* **1993,** *32*, 5769-5778.

38. Connelly, N. G.; Geiger, W. E., *Chem Rev.* **1996,** *96*, 877-910.

39. Vanasselt, R.; Gielens, E. E. C. G.; Rulke, R. E.; Vrieze, K.; Elsevier, C. J., *J Am Chem Soc.* **1994,** *116*, 977-985.

Appendix

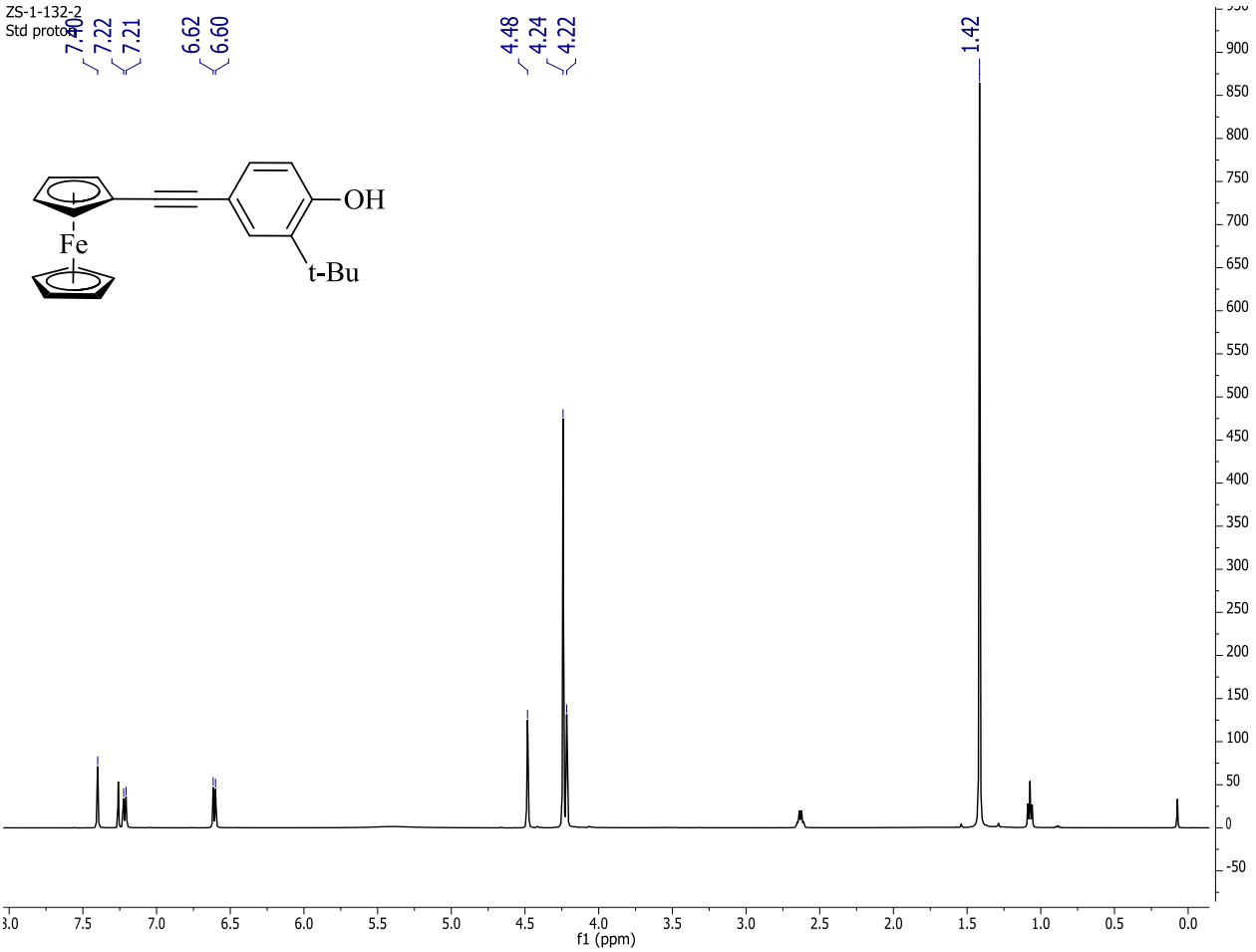


Figure A.1. ^{1}HNMR spectrum for compound **2.13**. Analysis was done on a Varian VNMRS 500 MHz and shifts are referenced to $CDCl_3$.

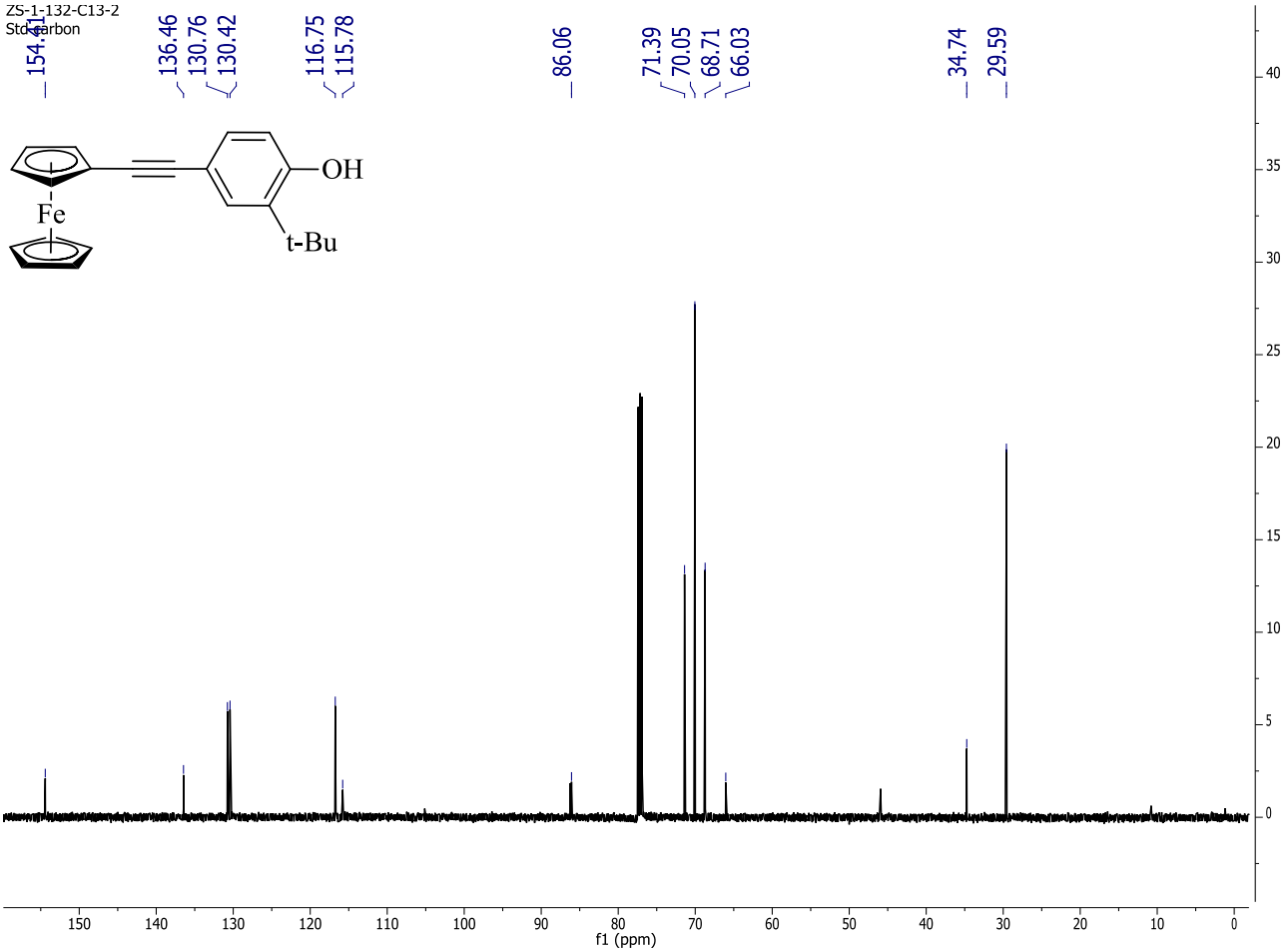


Figure A.2. ^{13}CNMR spectrum for compound **2.13**. Analysis was done on a Varian VNMRS 500 MHz and shifts are referenced to $CDCl_3$.

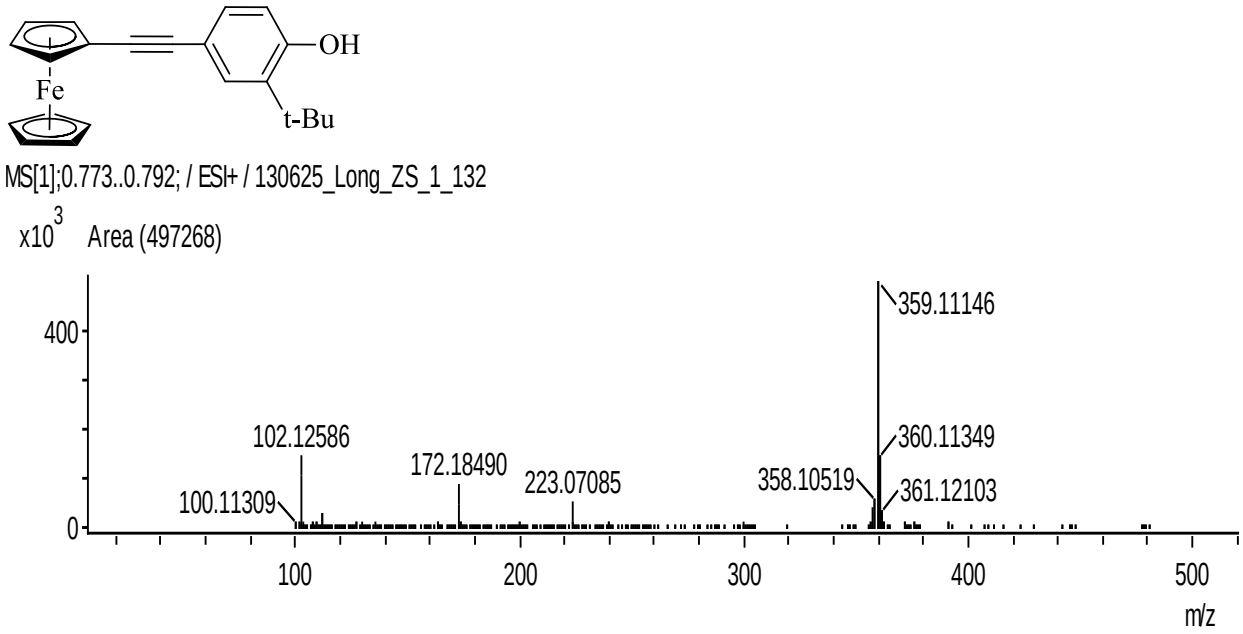


Figure A.3. DART-MS spectrum from compound 2.13 with a M + 1 peak of 359.11 m/z.

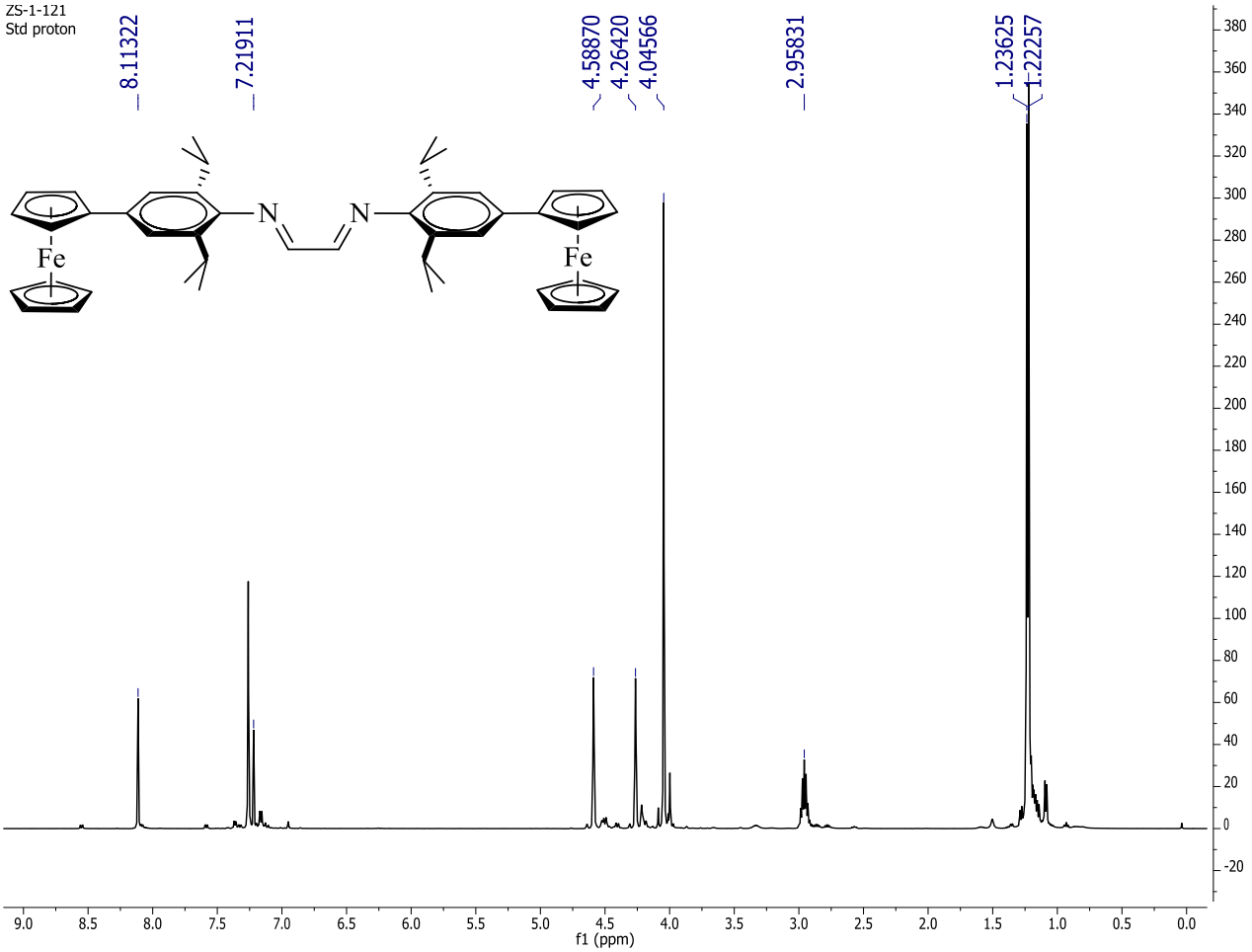


Figure A.4. ^{1}HNMR spectrum for compound **2.18**. Analysis was done on a Varian VNMRS 500 MHz and shifts are referenced to $CDCl_3$.

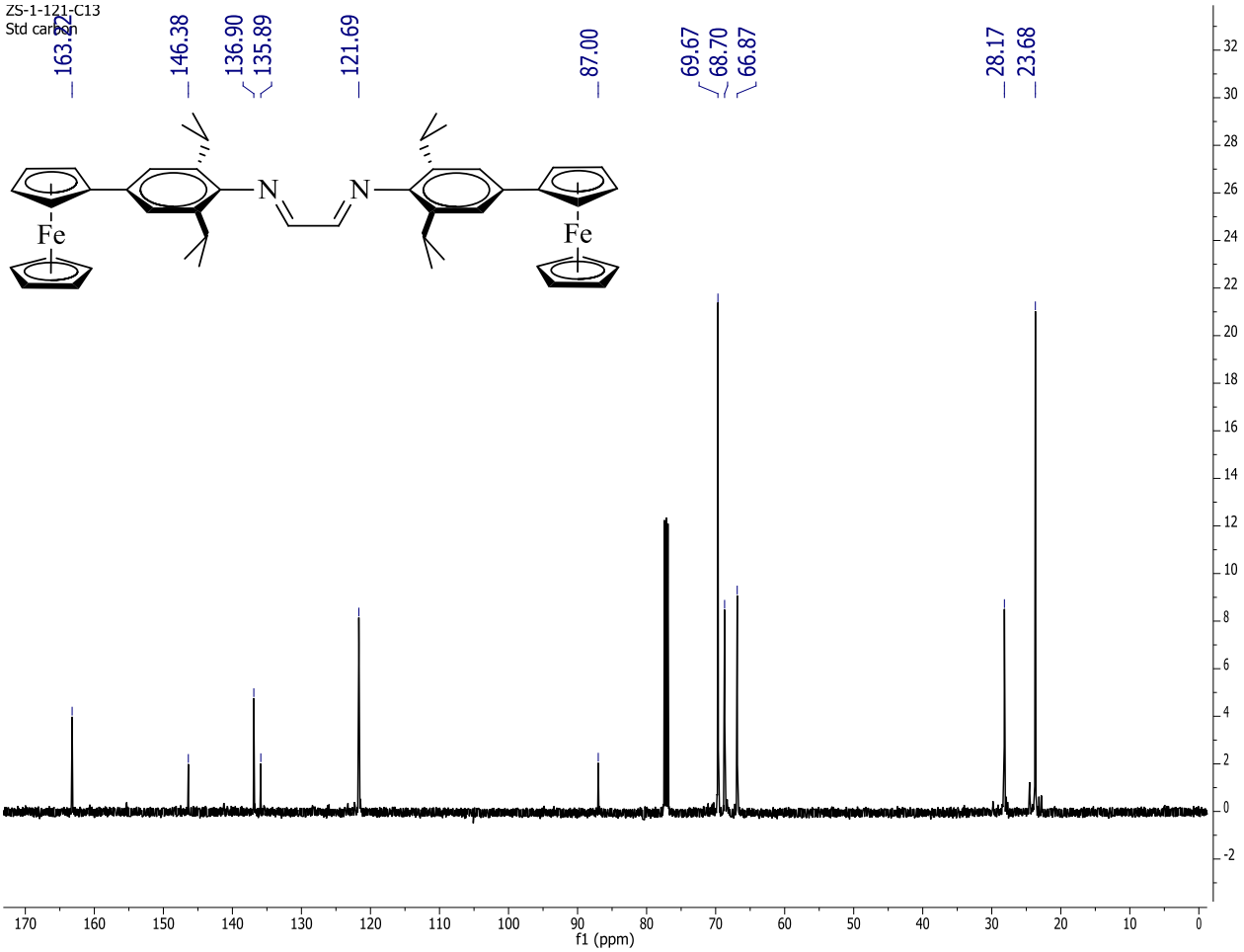


Figure A.5. ^{13}CNMR spectrum of compound **2.18**. Analysis was done on a Varian VNMRS 500 MHz and shifts are referenced to $CDCl_3$.

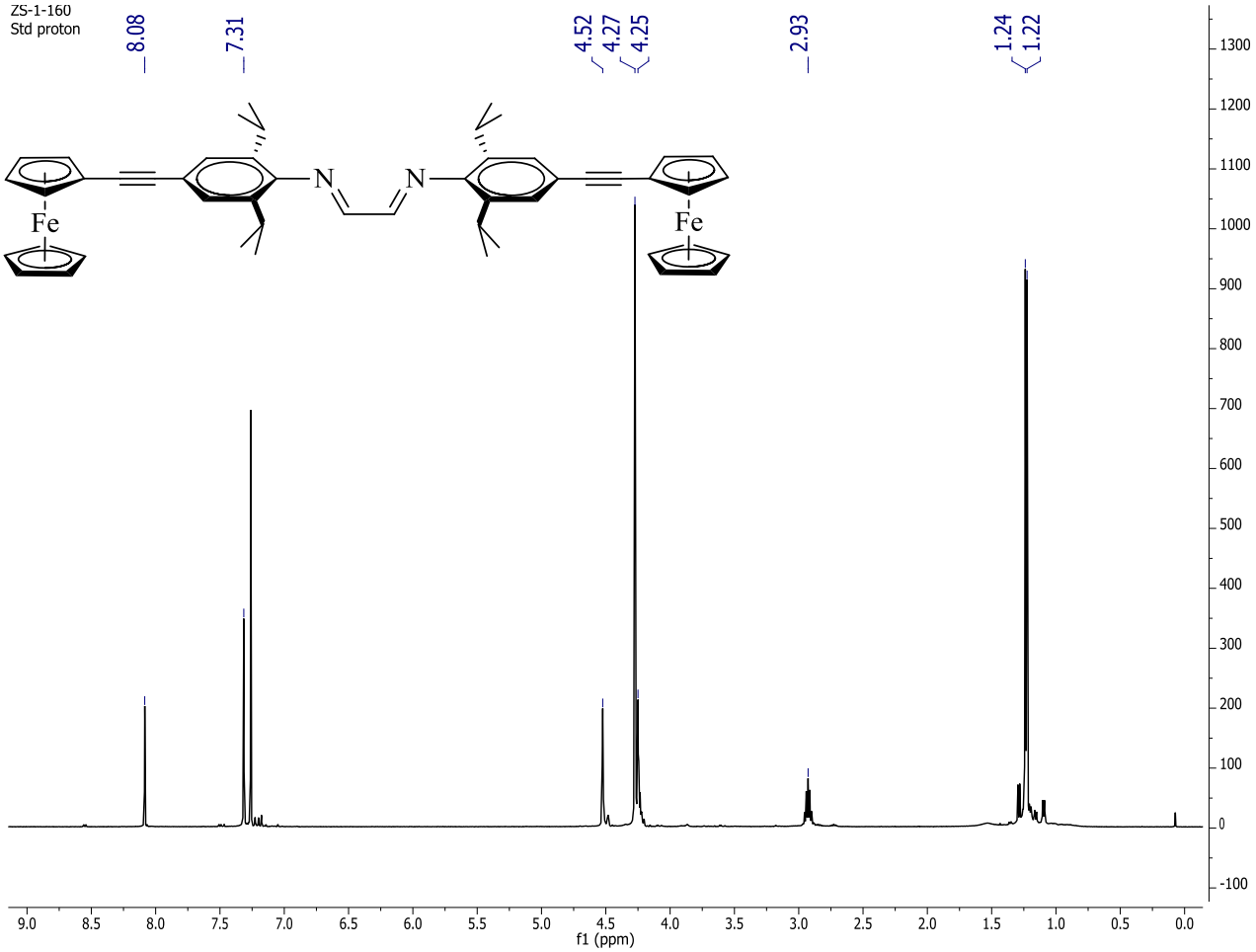


Figure A.6. ^{1}HNMR spectrum of compound **2.19**. Analysis was done on a Varian VNMRS 500 MHz and shifts are referenced to $CDCl_3$.

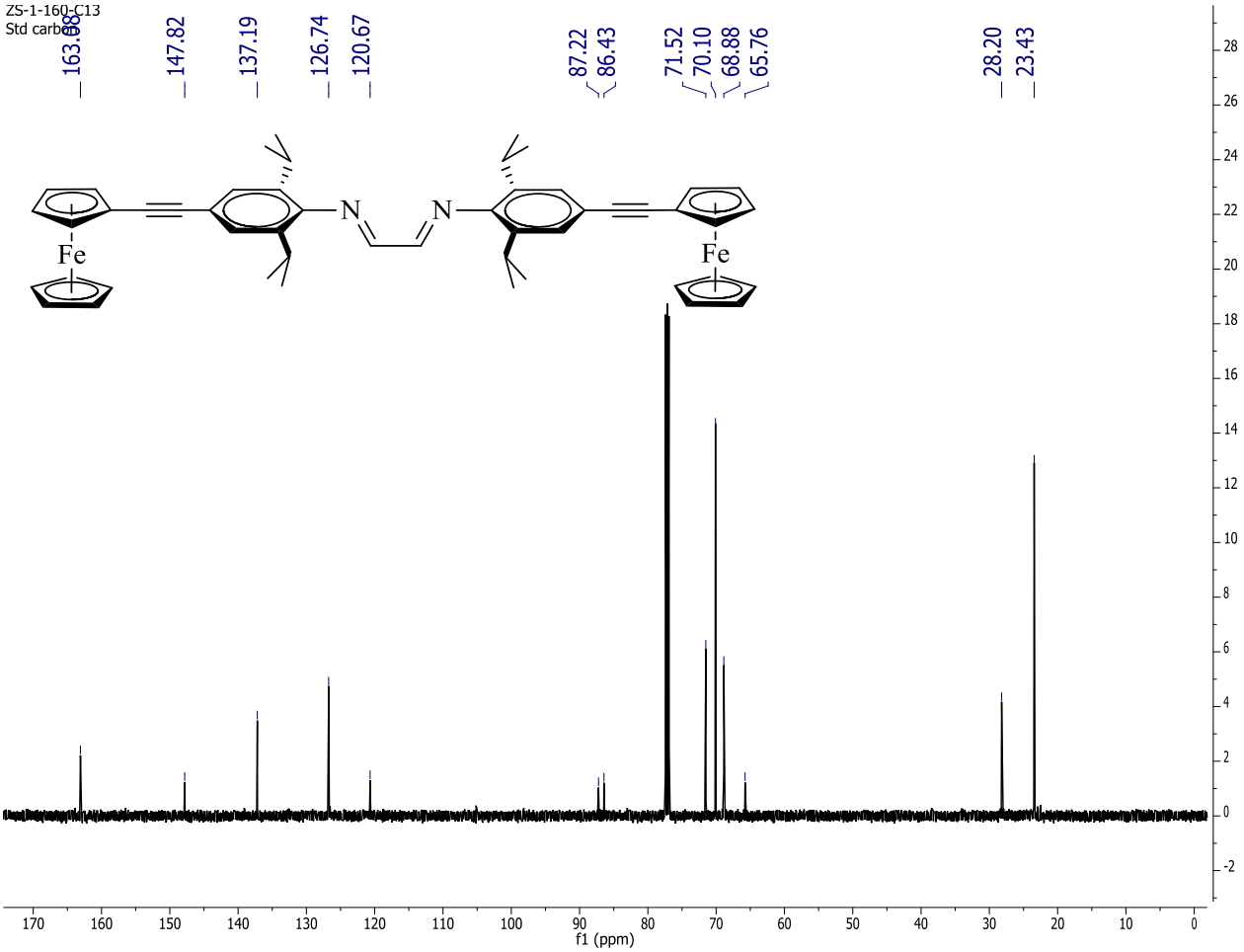


Figure A.7. ^{13}CNMR spectrum for compound **2.19**. Analysis was done on a Varian VNMRS 500 MHz and shifts are referenced to $CDCl_3$.

Vita

Zachary Reynolds Sprigler was born in New Albany, Indiana on August 18, 1988. After graduating from Floyd Central High School, he attended Butler University in Indianapolis, Indiana where he received his Bachelor of Science degree in Chemistry in May 2011. He then started his graduate studies in Chemistry at the University of Tennessee, Knoxville in August 2011.